AD 664127

TECHNICAL REPORT NO. 1-801

DEVELOPMENT OF ON-STRUCTURE STRESS GAGES

by

R. W. Faust
J. K. Ingram

November 1967

Sponsored by

Defense Atomic Support Agency

Conducted by

U. S. Army Engineer Waterways Experiment Station
CORPS OF ENGINEERS
Vicksburg, Mississippi

72

TECHNICAL REPORT NO. 1-801

DEVELOPMENT OF ON-STRUCTURE STRESS GAGES

by

R. W. Faust

J. K. Ingram

November 1967

Sponsored by

Defense Atomic Support Agency
NWET Subtask 11x13x03

Conducted by

U. S. Army Engineer Waterways Experiment Station
CORPS OF ENGINEERS
Vicksburg, Mississippi

ARMY-MRC VICKSBURG, MISS.

BLANK PAGE

THE CONTENTS OF THIS REPORT ARE NOT TO BE USED FOR ADVERTISING, PUBLICATION, OR PROMOTIONAL PURPOSES. CITATION OF TRADE NAMES DOES NOT CONSTITUTE AN OFFICIAL ENDORSEMENT OR APPROVAL OF THE USE OF SUCH COMMERCIAL PRODUCTS.

ABSTRACT

This report describes the development of three types of on-structure stress (OSS) gages (the IF and FS soil-pressure gages and the M-1 airblast gage) based upon the load column principle. The OSS gage design is based upon the assumption (backed by theory and experiment) that if the gage is made much stiffer than the soil, the overregistration of the gage approaches a constant value.

A brief discussion of some of the unique problems of measurement of soil pressures is presented.

Six OSS gages (four IF, one FS, and one M-1) were statically tested and evaluated with respect to linearity, hysteresis, resolution, thermal sensitivity, and strain sensitivity. Dynamic tests were performed in a laboratory shock tube and blast load simulator facilities.

The OSS gages are concluded to be adequate for soil-pressure measurements on certain types of rigid structures and for airblast measurements, even in explosive atmospheres. They successfully measured dynamic gas pressures up to 5,000 psi in the firing tubes of the laboratory blast simulator device.

Additional research is recommended to evaluate the gage performance more completely in static and dynamic soil tests. A range of soil types from coarse dry sand to moist fat clays should

be investigated. Future research on gages for measuring soil pressures on structures should be concentrated on development of small gages for use with models and thin-walled structures.

PREFACE

This investigation was conducted by the U. S. Army Engineer Waterways Experiment Station (WES) as a continuation of Nuclear Weapons Effects Tests Subtask 11x13x03 sponsored by the Defense Atomic Support Agency.

The work was conducted during the period 1962 through 1965 under the general supervision of Mr. G. L. Arbuthnot, Jr., Chief of the Nuclear Weapons Effects Division, and Mr. L. F. Ingram, Chief of the Physical Sciences Branch.

SP 5 R. W. Faust made the design calculations for the IF and FS gages. SP 5 R. Moore made the design calculations for the M-1 gage. Mr. J. K. Ingram performed the initial strain gage installation at WES and conducted some of the initial tests. Later in-house strain gaging was done by Mr. J. T. Kitchens of the Instrumentation Branch. The shock tube tests were performed by Mr. M. A. Vispi. PVT T. Buckley assisted with the data reduction. This report was written by SP 5 Faust and Mr. Ingram, under the direction of Mr. J. D. Day, Chief, Blast and Shock Section.

COL Alex G. Sutton, Jr., CE, and Mr. J. B. Tiffany were Director and Technical Director, respectively, of WES during the course of this investigation and the preparation of this report. COL John R. Oswalt, Jr., was Director during the final publication of this report.

CONTENTS

FIGURES

NOTATION

A Area, in^2

A_c Cross-sectional area of gage column, in^2

D Diameter of gage face, inches

D_o Outside diameter of gage, inches

e_i Input voltage, volts

e_o Output voltage, volts or mv

E Young's modulus for steel (compression), psi

E_c Modulus of gage (compression), psi

E_s Young's modulus for soil (compression), psi

f Gage factor

f_n Undamped natural frequency

F Total load on gage column, pounds

H One-half gage thickness, inches

L Length, inches

P Applied pressure, psi

P_m Measured stress, psi

P_{so} Applied surface pressure, psi

q Fluid stress, psi

Q Additive stress caused by gage rigidity, psi

r Radial distance, inches

R Electrical resistance, ohms

δ Deflection, inches

Δ Total deflection, inches

ϵ Strain, in/in

ϵ_a Apparent strain, in/in

ϵ_t Total true strain, in/in

ϵ_x Transverse strain, in/in

ϵ_y Axial strain, in/in

$\mu\epsilon$ Microstrain, 10^{-6} in/in

σ_y Axial stress, psi

υ Poisson's ratio

CONVERSION FACTORS, BRITISH TO METRIC UNITS OF MEASUREMENT

Multiply	*By*	*To Obtain*
QUANTITIES AND UNITS OF SPACE		
Length		
Inches	2.54 (exactly)	Centimeters
Feet	0.3048 (exactly)	Meters
Yards	0.9144 (exactly)	Meters
Miles (statute)	1.609344 (exactly)	Kilometers
Area		
Square inches	6.4516 (exactly)	Square centimeters
Square feet	0.092903 (exactly)	Square meters
Square yards	0.836127	Square meters
Square miles	2.58999	Square kilometers
Volume[a]		
Cubic inches	16.3871	Cubic centimeters
Cubic feet	0.0283168	Cubic meters
Cubic yards	0.764555	Cubic meters
Capacity[a]		
Fluid ounces (U.S.)	29.5737	Cubic centimeters
	29.5729	Milliliters[a]
Liquid pints (U.S.)	0.473179	Cubic decimeters
	0.473166	Liters[a]
Gallons (U.S.)	3.78543	Cubic decimeters
	3.78533	Liters[a]
Gallons (U.K.)	4.54609	Cubic decimeters
	4.54596	Liters[a]
Cubic feet	28.3160	Liters[a]
QUANTITIES AND UNITS OF MECHANICS		
Mass		
Grains (1/7000 lb avdp)	64.79891 (exactly)	Milligrams
Troy ounces (480 grains)	31.1035	Grams
Ounces (avdp)	28.3495	Grams
Pounds (avdp)	0.45359237 (exactly)	Kilograms
Short tons (2000 lb)	907.185	Kilograms
	0.907185	Metric tons
Long tons (2240 lb)	1016.05	Kilograms
Force/Area		
Pounds per square inch	0.070307	Kilograms per square centimeter
	0.689476	Newtons per square centimeter
Pounds per square foot	4.88243	Kilograms per square meter
	47.8803	Newtons per square meter
Mass/Volume (Density)		
Ounces per cubic inch	1.72999	Grams per cubic centimeter
Pounds per cubic foot	16.0185	Kilograms per cubic meter
	0.0160185	Grams per cubic centimeter
Tons (long) per cubic yard	1.32894	Grams per cubic centimeter
Mass/Capacity		
Ounces per gallon (U.S.)	7.4893	Grams per liter[a]
Ounces per gallon (U.K.)	6.2362	Grams per liter[a]
Pounds per gallon (U.S.)	119.829	Grams per liter[a]
Pounds per gallon (U.K.)	99.779	Grams per liter[a]
Bending Moment or Torque		
Inch-pounds	0.011521	Meter-kilograms
	1.12985×10^6	Centimeter-dynes
Foot-pounds	0.138255	Meter-kilograms
	1.35582×10^7	Centimeter-dynes
Foot-pounds per inch	5.4431	Centimeter-kilograms per centimeter
Ounce-inches	72.008	Gram-centimeters
Velocity		
Feet per second	30.48 (exactly)	Centimeters per second
Miles per hour	1.609344 (exactly)	Kilometers per hour
	0.44704 (exactly)	Meters per second
Flow		
Cubic feet per minute	0.4719	Liters[a] per second
Gallons (U.S.) per minute	0.06309	Liters[a] per second

[a] Laboratory volumetric apparatus in the United States is calibrated in milliliters rather than cubic centimeters (1 ml = 1.000028 cm^3). The difference (28 ppm) is seldom of consequence.

CHAPTER 1

INTRODUCTION

1.1 OBJECTIVE

The general objective of this study was to develop reliable gages for measuring static and dynamic stresses induced on buried structures and structural elements by mechanical loading. Emphasis was on the measuring of free-field (soil) stresses to aid in the design of hardened complexes and structural elements that must resist the loading effects of explosions.

1.2 SCOPE

This report describes the design and evaluation of three on-structure stress (OSS) gage types based upon the end-loaded piston principle. These gage types are designated the IF, FS, and M-1 gages. Theoretical background, design equations, and evaluation tests and results are discussed. The IF gage, which is the basic product of this investigation, receives primary attention.

1.3 BACKGROUND

In March 1963 the first of a new series of OSS gages was designed and built at the Waterways Experiment Station (WES). This gage is essentially a load cell calibrated to measure pressure and intended to be flush-mounted in the outside wall, floor, or roof of

a buried structure. It is modeled after the WES aluminum cell (Reference 1), which was designed to measure pressures on buried concrete structures, but was different in size and compressibility. The aluminum cell was designed to deform as the surrounding structural concrete deforms. The OSS gage, on the other hand, was made to be very much stiffer than most structural materials. This avenue of attack on the soil-structure interaction problem was suggested in Reference 2, relying upon the work described in References 3, 4, 5, and 6, and using Boussinesq's overregistration equations (Reference 7).

The overregistration of a buried gage is believed to be due to the phenomenon, common in granular soils, of a redistribution of stresses at the gage-soil interface called "arching." Arching action of soils has been studied by numerous investigators, but thus far no really reliable method has been found for quantitatively predicting its effect. Although arching is more serious in soils, it can occur even in less complicated media. For example, the redistribution of stresses as a result of arching in the vicinity of a disk-shaped pressure cell embedded in an elastic, homogeneous, isotropic medium was considered in Reference 4. While the results are not directly applicable to soil, they do indicate the importance of the ratio of the moduli of the soil and cell as a factor influencing the registration errors of the gage. More specifically, Figure 1.1 shows the

theoretical relation which exists for two types of disk-shaped free-field gages; namely, those in which the entire gage compresses axially (total area) and those in which only the central portion of the gage deforms (central area) as in the numerous diaphragm cells which have been developed. For an OSS gage mounted flush in the wall of a buried structure, the diameter-to-thickness ratio of the gage approaches infinity since the thickness of the gage is practically zero. Such gages, therefore, should not be subject to errors as a result of changes in diameter as are the free-field gages.

However, registration errors of both free-field and OSS gages may also be due to the fact that, in general, the gage cannot be made to deform exactly as would the material which the gage replaces. Thus, a redistribution of stress occurs at the gage-soil interface. For gages which are stiffer than the soil, this redistribution is probably similar to that shown in Figure 1.2. Values of Young's modulus E_s in compression for various soils vary considerably but are roughly 5×10^3 to 22×10^3 psi for sand and near 0 to 7×10^3 psi for clay.[1] Thus, the ratio of soil modulus to gage modulus E_s/E_c for a very stiff gage (with a modulus of, say, 11×10^6 psi) will vary between $22 \times 10^3/11 \times 10^6 = 2 \times 10^{-3}$ and nearly zero; in

---

[1] A table of factors for converting British units of measurement to metric units is presented on page 11.

other words, the gage is very much stiffer than any soil in which it might be placed. For this reason, registration errors of the gage due to the inequality of moduli should be relatively insensitive to variations in soil modulus, even variations on the order of two- or threefold. This is essentially the conclusion reached in Reference 2. Further, it is contended that if the gage stiffness E_c is very much greater than the soil stiffness E_s the gage will overregister by a constant percentage of the true soil pressure. In the case of the Road Research Laboratory (RRL) gage embedded in well-compacted silty clay, overregistration was found to be a constant 10 percent for nonshocked dynamic loadings of applied pressure levels under 50 psi. The design of the OSS gages discussed in this report is based on the assumption that gages much stiffer than the soil in which the structure is placed will also overregister at a constant rate.

1.4 DESCRIPTION OF GAGES

As previously mentioned, the design of the OSS gage is very similar to that of the WES aluminum cell except that the OSS gages are intended to be as stiff as possible. The cells are designed for a pressure of 500 psig, but due to their rigidity they can be loaded to pressures as high as approximately 20,000 psi without damage.

Three gage types were developed in the course of this

investigation. In chronological order of development they are: (1) IF gage, (2) FS gage, and (3) M-1 gage.

The IF gage is approximately 3 inches long by 1.4 inches in diameter, made of stainless steel, and designed for mounting in thick-walled structures.

The FS gage is quite similar to the IF gage, but it is designed for mounting in smaller, thinner walled structures and is therefore smaller. The gage is made of aluminum and is 1.75 inches long by 0.5 inch in diameter.

The M-1 gage was designed for measuring either airblast pressure or soil stress on a structure, and was designed to have greater sensitivity than the other gage types. It is made of stainless steel and is approximately 1.8 inches long by 1.0 inch in diameter.

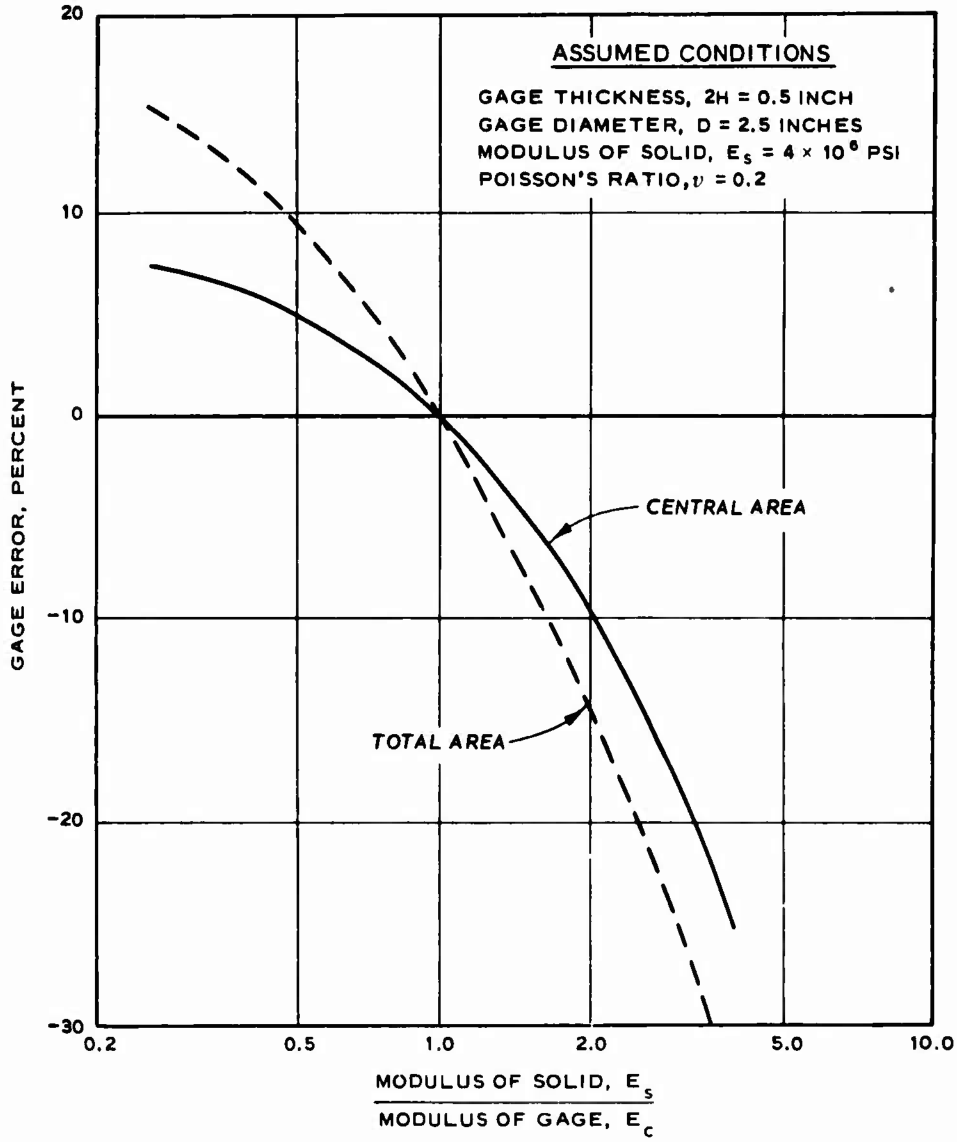

Figure 1.1 Theoretical relation of moduli ratio to gage registration. Total-area axial compression and central-area axial compression for disk-shaped free-field stress gages (Reference 4).

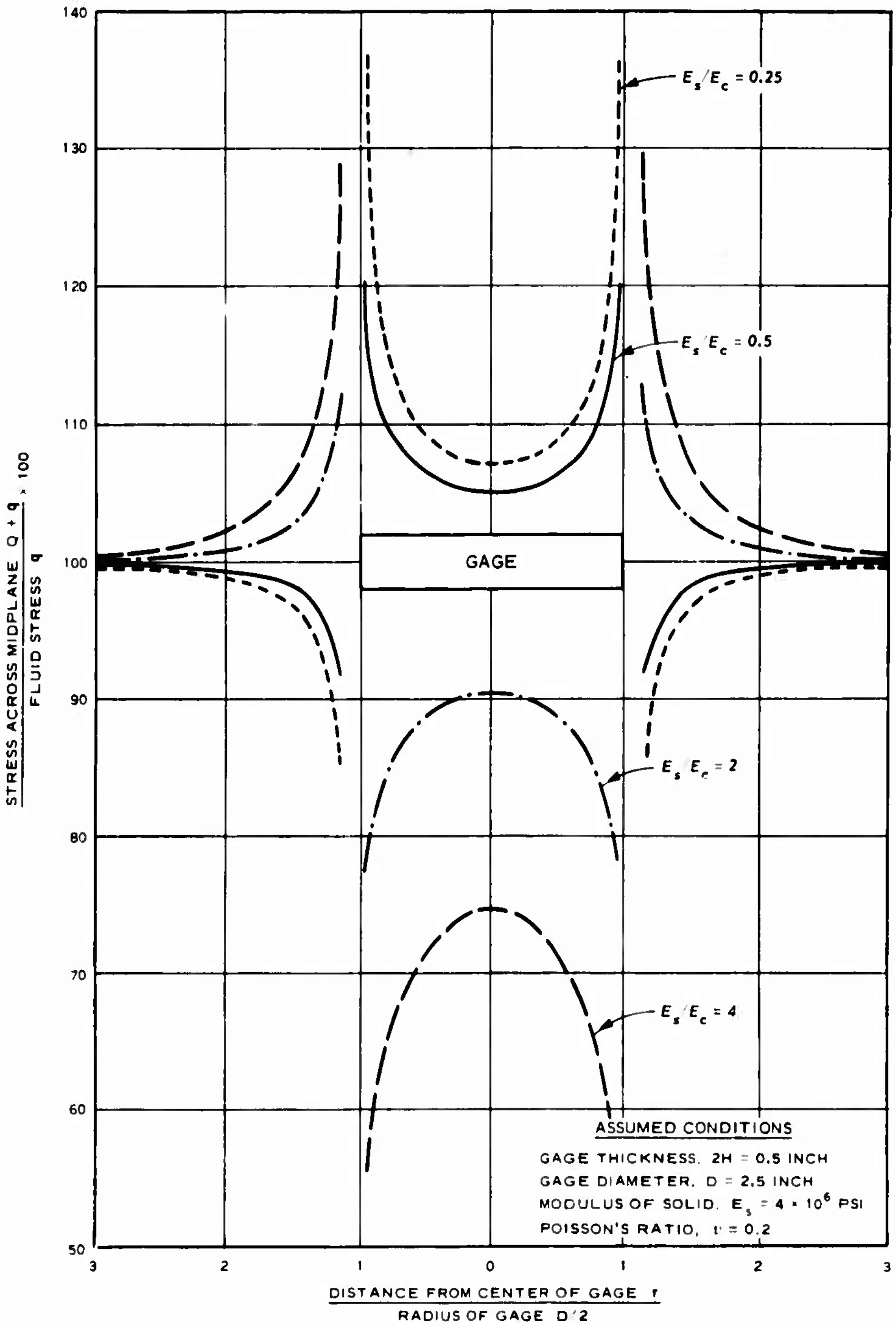

Figure 1.2 Effect of the ratio of elastic moduli of gage and surrounding media on stress distribution (Reference 4).

CHAPTER 2

GENERAL DESIGN REQUIREMENTS AND DESIGN CALCULATIONS

2.1 GENERAL DESIGN REQUIREMENTS

Limitations on the size and shape of OSS gages are not nearly so restrictive as they are for free-field gages. It is generally desirable to design the gage so that it can be installed from within a buried structure; therefore, such gages have usually been made cylindrical with a threaded outer case.

Remote readout of OSS gages, while not always essential, is a highly desirable feature. When it is necessary to monitor the gage from a distance or to measure dynamic stresses, conversion of the gage deformation into an electrical signal is required. This can be accomplished in numerous ways. For the gages discussed in this report, the electrical signal is produced by bonded strain gages.

Soil pressure gages must be rugged enough to withstand compaction shocks, the abrasion of soil and rock, strong inertial forces, the presence of moisture and dust, and sometimes wide variations in temperature, even under laboratory conditions. Placement of gages and deposition of the soil around them have been found to be of paramount importance in obtaining reliable readings. Even in the laboratory, no completely satisfactory method has yet been devised

to insure uniform soil conditions before beginning a given test. The considerable scatter present in almost all soil pressure data is often the result of the difficulties associated with gage and soil placement.

In field use these difficulties are even more pronounced. Thus, the ideal field OSS gage should be rugged, impervious to moisture and other contaminants, and, further, should maintain its zero point and calibration over rather long periods of time, sometimes as much as 15 to 20 years, especially for long-term static tests.

It is desirable also that the gage be capable of responding to both static and dynamic pressures. Piezoelectric transducers, such as the RRL gage, are not well suited to measuring static loads. The semiconductor strain gages used as the sensing elements of the OSS gages are piezoresistive devices which are useful for both types of loading. The natural frequency of the larger developmental gage (IF gage) is in the range of 40,000 Hz, making it suitable for measuring impulse loads with rise times of a few microseconds.

2.2 DESIGN CALCULATIONS

The basic design technique is applicable for all gage types discussed in this report, and is, therefore, presented in detail only for the IF gage.

2.2.1 Induced Strain. Assuming the active area, i.e. the gage

face, to be a circle with a diameter D of 3/4 inch, the total load F on the gage column for the 500-psi design pressure will be

$$F = \frac{500\pi D^2}{4} \tag{2.1}$$

or

$$F = 220.9 \text{ pounds}$$

The gage column is instrumented with four semiconductor strain gages arranged in a full bridge, with two of the gages sensing axial strain ϵ_y and two sensing transverse strain ϵ_x. In order to get an approximate idea of the resolution of the cell, let it be assumed that the output signal is read, without amplification, on a commercial strain indicator. Such indicators can ordinarily be read directly to the nearest 5×10^{-6} in/in, or 5 $\mu\epsilon$, apparent strain. If it is desired to resolve 1 psi, then the gage dimensions must be such that a pressure of 1 psig applied to the gage face results in at least 5 $\mu\epsilon$ apparent strain, which is equivalent to 2,500 $\mu\epsilon$ at 500 psig. In order to be certain of achieving at least 1-psi resolution, this figure was doubled for the IF gage; that is, it is designed to have an apparent strain output of 5,000 $\mu\epsilon$ at an applied pressure of 500 psig.

Let ϵ_a represent the apparent strain or indicator reading and let ϵ_t represent the total true strain output of the bridge circuit. Then, with the indicator gage factor dial set on 2.00, the

following relation obtains between ϵ_a and ϵ_t .

$$\epsilon_t = \epsilon_a \frac{\text{Gage factor dial setting}}{\text{Gage factor(s) of bridge}} \tag{2.2}$$

or

$$\epsilon_a = \epsilon_t \frac{\text{Gage factor(s) of bridge}}{\text{Gage factor dial setting}} \tag{2.3}$$

The indicators used for the first IF gage made were P-type, silicon, semiconductor gages from a single lot, with an unstrained resistance R of 338 ohms (±1 percent) and a gage factor f of 121 (±2 percent). Thus, for these gages, $\epsilon_t = \epsilon_a\ 2.00/121$ or, for 5,000 $\mu\epsilon$ output, $\epsilon_t = (5{,}000)(2.0)/121 = 82.6\ \mu\epsilon$. Because the commercial strain indicator readout devices are designed for use with 120-ohm strain gages, readings should be corrected for gages having resistance other than 120 ohms. However, for 350-ohm gages this correction is small, about 0.3 percent, and is neglected.

With the four gages arranged as described above, the total bridge output is

$$\epsilon_t = 2\epsilon_y + 2\epsilon_x \tag{2.4}$$

Since $\epsilon_x = \upsilon\epsilon_y$, where υ = Poisson's ratio for stainless steel $\cong 0.33$

$$\epsilon_t = 2\epsilon_y + 2\upsilon\epsilon_y \tag{2.5}$$

or $\epsilon_y = \frac{\epsilon_t}{2 + 2\upsilon} = 82.6/2.66 = 31.1\ \mu\epsilon$ and $\epsilon_x = -\upsilon\epsilon_y = -(0.33)(31.1) = -10.3\ \mu\epsilon$. The axial stress σ_y in the column required to produce strain $\epsilon_y = 31.1\ \mu\epsilon$ is

$$\sigma_y = E\epsilon_y \tag{2.6}$$

where E is Young's modulus for steel. Since $E = 29 \times 10^6$ psi, $\sigma_y = (29 \times 10^6 \text{ psi})(31.1 \times 10^{-6} \text{ in/in}) = 908$ psi.

Knowing the load F and stress σ_y , the cross-sectional area A_c of the column can be determined by

$$A_c = \frac{F}{\sigma_y} = \frac{220.9 \text{ pounds}}{908 \text{ psi}} = 0.243 \text{ in}^2 \tag{2.7}$$

Assuming the column to be square, its dimensions will be $(0.493 \text{ in})^2 = 0.243 \text{ in}^2$.

As a result of some approximations in the original design calculations, the gage column actually measures 0.480 inch on a side, which makes the cross-sectional area $A_c = 0.230 \text{ in}^2$, $\sigma_y = 961$ psi, $\epsilon_y = 33.1\ \mu\epsilon$, $\epsilon_x = -10.9\ \mu\epsilon$. These dimensions result in an apparent strain output of $\frac{121}{2}(66.2 + 21.8) = 5{,}324\ \mu\epsilon$ at 500 psig.

2.2.2 Deflection of Gage Column. As illustrated in Figure 2.1a, the gage column consists of an O-ring just below the loading face, a square portion to which the gages are attached, and a circular base through which the strain gage lead wires exit.

The total gage column deflection can be estimated by considering each of the segments of the column to compress axially by the amount

$$\delta_i = \frac{FL_i}{A_i E} \tag{2.8}$$

where δ_i = deflection of segment, inches

F = total load = 220.9 pounds

L_i = length of segment, inches

A_i = Cross-sectional area of segment, in^2

E = Young's modulus for steel = 29×10^6 psi

The total deflection of the gage column, relative to the gage body, is then

$$\Delta_c = \sum \delta_i = \sum \frac{FL_i}{A_i E} = \frac{F}{E} \sum \frac{L_i}{A_i} \tag{2.9}$$

For these calculations the gage column form is somewhat simplified and is assumed to have the dimensions shown in Figure 2.1a. Thus

$$\Delta_c = 2\delta_1 + \delta_2 + \delta_3 + \delta_4 \tag{2.10}$$

and

$$2\delta_1 = \frac{2(220.9 \text{ pounds})(0.08 \text{ inch})}{(0.442 \text{ in}^2)E} \simeq \frac{80.0}{E}$$

$$\delta_2 = \frac{(220.9 \text{ pounds})(0.15 \text{ inch})}{(0.259 \text{ in}^2)E} \simeq \frac{128.0}{E}$$

$$\delta_3 = \frac{(220.9 \text{ pounds})(1.00 \text{ inch})}{(0.230 \text{ in}^2)E} \cong \frac{962.0}{E}$$

$$\delta_4 = \frac{(220.9 \text{ pounds})(0.374 \text{ inch})}{(0.601 \text{ in}^2)E} \cong \frac{137.5}{E}$$

$$\Delta_c = \frac{(80.0 + 128.0 + 962.0 + 137.5) \text{ lb/in}}{29 \times 10^6 \text{ psi}}$$

$$\Delta_c = 45.1 \times 10^{-6} \text{ inches} = 0.0000451 \text{ inch}$$

The diameter-deflection ratio is equal to $\dfrac{0.750 \text{ inch}}{45.1 \times 10^{-6} \text{ inches}}$ $\cong 16,630$. The modulus of deformation E_c for the gage is

$$E_c = \frac{PD_o}{\Delta_c} \tag{2.11}$$

where P = applied pressure, psig

D_o = outside diameter of gage = 1.375 inches

Δ_c = 45.1×10^{-6} inches

$$E_c = \frac{(500 \text{ psig})(1.375 \text{ inches})}{45.1 \times 10^{-6} \text{ inches}} = 15.2 \times 10^6 \text{ psig}$$

Thus the IF gage is about 43 percent stiffer than the RRL gage.

2.2.3 Electrical Aspects. As noted in the previous section, the strain gages are bonded to the square portion of the gage column with two gages parallel to the longitudinal axis of the column and two to the transverse axis (Figure 2.1b). Connecting the gages in

a Wheatstone bridge with the longitudinal (compression) gages in opposite legs affords two important advantages. First, the full bridge configuration provides nominal temperature compensation, and therefore the minimum in additional balance resistors or temperature sensing elements is required. In general, such additional resistances reduce the bridge sensitivity. Second, the arrangement of the gages on the gage column automatically cancels out any signal due to bending-induced strain. Thus, the gage output is proportional only to the normal force component on the gage face. In any case, tangential forces on the face plate are not likely to be large when the cell is mounted flush. Assuming the unstrained resistance of all four gages to be 338 ohms, the open circuit bridge output voltage e_o at 500-psig applied pressure will be

$$e_o = \frac{e_i f \epsilon_t}{4} \tag{2.12}$$

where e_i is the input voltage and f is the gage factor. The specific output then is

$$\frac{e_o}{e_i} = \frac{f\epsilon_t}{4} = \frac{(121)(66.2 + 21.8) \times 10^{-6}}{4} = 2.66 \times 10^{-3} \text{ v/v} \tag{2.13}$$

or 2.66 mv output per volt input at 500 psig.

If the readout equipment used is something other than a strain indicator, which normally provides an input of about 3 volts, the

input voltage which may be applied to the bridge will depend upon the power (heat) dissipating ability of the gage installation. The gage column is a good heat sink, and therefore the manufacturer's recommendation that the gage current not exceed 30 ma should be conservative. Allowing this maximum current input results in maximum input voltage of about 20 volts. However, 10 volts should give adequate output for most purposes.

The optimum desired sensitivity was defined as not less than 20-mv output at an applied pressure of 500 psig and an input voltage of 10 volts. This sensitivity results in a theoretical apparent strain output of approximately 3,900 $\mu\epsilon$ full scale on an SR-4 strain indicator at a gage factor setting of 2.0.

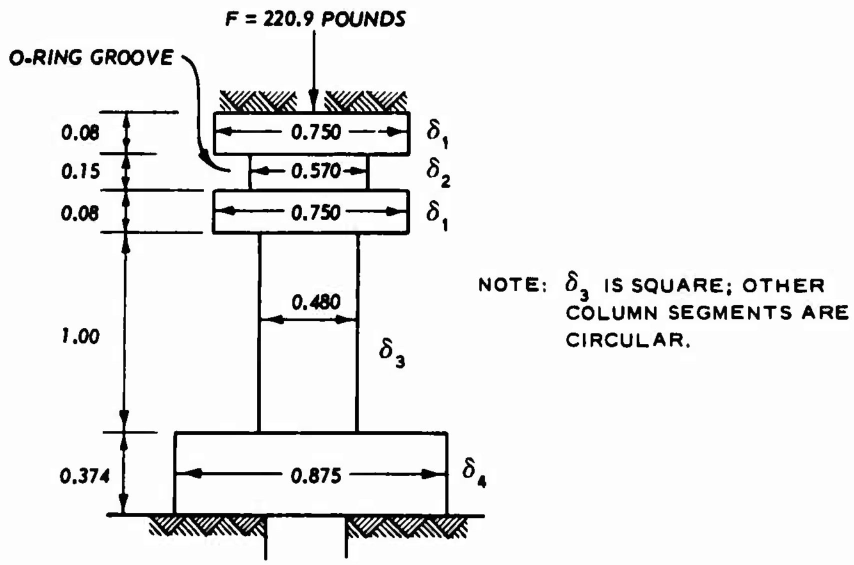

a. Gage column dimensions (inches).

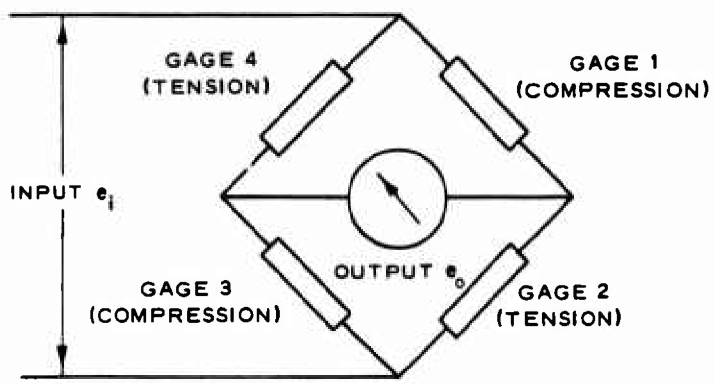

b. Electrical schematic.

Figure 2.1 Gage column dimensions and electrical schematic of gage arrangement on column.

CHAPTER 3

CONSTRUCTION AND EVALUATION OF GAGES

3.1 IF GAGE

The first IF gage (IF-1-WES) was made at the WES. Figure 3.1 is a machine drawing. Figure 3.2 shows Gage IF-1-WES along with its strain gages before and after assembly. The first gage differs slightly from the later models in that it is not fitted with an electrical connector. Figure 3.3 shows the intended locations of the strain gages on the column, and Figure 3.4 shows the mounted gages before and after gage coating. The strain gages were bonded to the column using an epoxy adhesive.

3.1.1 Thermal Effects. Before the gage coating was applied, it was noticed that the bridge output drifted considerably. This drift was caused by three separate factors: incomplete cure of the adhesive, temperature sensitivity of the gages because of imperfect temperature compensation, and sensitivity of the strain gages to ambient light. The light sensitivity completely disappeared after application of several coats of opaque moistureproofing compound. However, the temperature-induced zero shift persisted. A day later, plots (Figure 3.5) of temperature versus time and bridge output versus time over the same 6-hour period were made. The similarity in shape of the two curves seemed to indicate that the zero drift

problem was primarily, if not completely, due to temperature changes. This first drift check was made at room temperature. Later, the gage was placed in a small laboratory oven and checked over a somewhat wider temperature range, as were the gages discussed below.

This temperature sensitivity made it difficult to calibrate Gage IF-1-WES. It was finally found necessary to place the gage in the oven along with a small calibration chamber in order to insure reasonably constant temperature. The full-scale output was about 4,900 $\mu\epsilon$, somewhat less than the predicted value of 5,324 $\mu\epsilon$ but still adequate, and exhibited reasonably good linearity.

3.1.2 Gage Construction by WES and Commercial Firms. In May 1963, the decision was made to build several more IF gage assemblies and to send four of these to commercial strain gage manufacturers who offered precision-gaging services. Experience with semiconductor strain gages indicated, particularly with respect to temperature compensation, that the manufacturers, with their greater selection of matched gages and personnel trained in strain gaging techniques, would have a much better chance of successfully gaging the transducer.

Requests for quotations were sent to the following companies: (1) Baldwin-Lima-Hamilton (BLH) Corporation, Electronics Division,

Waltham 54, Massachusetts, (2) Kulite-Bytrex (KB) Corporation, 50 Hunt Street, Newton 58, Massachusetts, (3) Micro Systems, Inc. (MSI), 170 North Daisy Avenue, Pasadena, California, and (4) Texas Instruments, Inc., 3609 Buffalo Speedway, Houston, Texas. The first three companies replied with quotations; Texas Instruments, Inc., declined.

Gage bodies were then sent to the three firms and returned to the WES in the months following. The four gages subsequently tested (IF-1-WES and the three gaged by the other agencies) were:

Gage	Gaged by	Connector	Column Material
IF-1-WES	Waterways Experiment Station	None	17-4ph
IF-2-BLH	Baldwin-Lima-Hamilton	Amphenol	Ni^{39}
IF-5-KB	Kulite-Bytrex	Amphenol	17-4ph
IF-6-MSI	Micro Systems, Inc.	Amphenol	17-4ph

The gage bodies and columns were all made of 17-4ph (precipitation hardened) stainless steel except for IF-2-BLH which has a $nickel^{39}$ alloy gage column. Each completely assembled gage weighed approximately 1.3 pounds and measured 1-3/8 inches in diameter by 3-1/2 inches long overall, exclusive of connecting

cable. As a matter of convenience, as well as to prevent damage to the strain gages, all gages built after IF-1-WES were fitted with electrical connectors. The connectors used were not hermetically sealed, and entrainment of pressure and consequent differential loadings could result if the gage were not properly mounted.

Often in pressure transducers measuring dynamic loads, electrical connections are a source of considerable noise. This has not proven to be a serious problem in this instance.

<u>3.1.3 Calibration Tests</u>. Upon receipt, all gages were checked to assure continuity and ample resistance to ground. Five separate calibration tests were used to evaluate the gages with respect to the following performance characteristics: (1) sensitivity or full-scale output, (2) temperature effect on sensitivity, (3) linearity, (4) hysteresis, (5) temperature effect on zero point, and (6) repeatability. Results are given in Table 3.1. In addition, a separate, no load, zero drift check was run on each gage.

Zero drift with temperature was checked over the range from room temperature (about 70 F normally) to 150 F. This was done in a small laboratory oven having a maximum temperature of about 600 F and capable of maintaining a constant temperature to

within ± 2 F. Readout equipment consisted of a commercial strain indicator and a switch-and-balance unit. The gage to be checked was placed in the oven and allowed to remain overnight. The following day the initial temperature and gage output were recorded and heating was begun. The heating rate was approximately $13^{\circ}F/hr$, and readings were taken at 15-minute intervals. Results of the zero drift test are shown in the composite plot of Figure 3.6. Notice that the IF-5-KB gage exhibits very much less sensitivity to temperature than do any of the other IF gages.

Calibration 1, to determine sensitivity or full-scale output, was conducted in a small pressure chamber built for this purpose. The chamber consists of two cylindrical, stainless steel sections with an O-ring seal between them. One section is threaded to receive the IF gage, the other to receive a 1/4-inch NPT pressure inlet. The cell was loaded in 50-psi increments from 0 to 600 psi and then unloaded in 100-psi steps. A typical pressure-output curve is shown in Figure 3.7a. The theoretical full-scale output, 5,324 $\mu\epsilon$, corresponds to a relative output of 2.57 mv/v.

With those gages having considerable zero drift, the entire calibration chamber was placed inside the oven in an attempt to maintain constant ambient temperature. In all cases, the temperature was recorded at each pressure reading. Calibration 1 was

repeated but with the introduction of a thin surgical rubber membrane over the face of the gage. The membrane was found to have no appreciable effect on the gage output in all cases.

An attempt to assess the effects of concentrated loads directly on the gage face, such as might occur in soils containing gravel, was made on one of the gages. The gage was loaded with a concentrated dead load at its center equivalent to various uniform pressures up to approximately 16,000 psi. A plot of the resultant data (Figure 3.7b) shows a linear gage output throughout this range.

Calibration 2, to determine the effect of temperature on gage sensitivity, was conducted by performing Calibration 1 at an elevated temperature, 100 F or greater. The change in slope of the calibration curve from Calibration 1 to Calibration 2, due essentially to a change in gage factor f of the strain gages, is taken as the sensitivity change.

Calibrations 3, 4, 5, and 6 were conducted by standard methods. The results are shown in Table 3.1.

3.1.4 Shock Tube Tests. The dynamic responses of the IF gage were investigated in a shock tube. Typical records from several tests are given in Figure 3.8. The gages were compared to a piezoelectric accelerometer to determine shock-induced vibration characteristics along both axes of the gage. Accelerometers were mounted

(1) directly on the end plate of the shock tube (Figure 3.8a), and (2) directly on the gage housing (Figure 3.8b). The IF gage was also compared to a parallel-mounted, commercial, fluid pressure transducer to determine waveform and amplitude characteristics (Figure 3.8c).

The oscillation seen in Figure 3.8a appears to be related to the mounting condition. The axial accelerometer mounted directly on the end plate parallel with the stress gage exhibits the same basic frequency as the stress gage.

Direct comparison between the developmental gage and a commercial, fluid pressure transducer (Figure 3.8c) yielded similar results. Amplitudes of the first peaks agreed within 8 psi, and the second peaks were in agreement to within 1 psi. These data indicate that static calibration can be used as a basis for dynamic testing.

Rise times were determined to be of the order of 5 or 6 μsec, and the undamped natural frequency f_n was found to be greater than 40,000 Hz.

3.1.5 Firing Tube Tests. Four dynamic tests were made with Gage IF-5-KB mounted in the end cap of a firing tube in the Small Blast Load Generator (SBLG), Reference 8. The SBLG and its appurtenances are described in detail in Reference 9. The firing tubes are loaded with line charges of primacord explosive. This cord explosive runs the length of each of the two firing tubes (Figure 3.9) and is center-detonated by electrical blasting caps. The ends of the

primacord bundles practically touch the firing tube end caps. Gas temperatures within the firing tubes reach several thousand degrees Fahrenheit within a few milliseconds. Attendant accelerations are of the order of 20,000+ g's; thus, an extremely rigorous environment exists for obtaining reliable pressure measurements. The transducer must have sufficient mass or compensating circuits to allow thermal insulation for adequate time resolution, and must be sufficiently insensitive to high accelerations of microseconds rise time. Although the IF gages do show temperature sensitivity for long-term measurements, the gages have excellent stability for short-duration thermal shocks due to the mass of the sensing column and location of the strain gages. Additionally, IF gages are quite insensitive to axial acceleration.

The IF gage pressure-time histories for three dynamic loadings in the firing tubes are shown in Figure 3.9. These measurements are considered to be excellent. A commercial gage of 60,000-psi range failed on the first attempt to measure pressures in the firing tube. Unfortunately, IF-5-KB was damaged during the last dynamic test. Although the reason for the failure is not known, it is believed that the load column was allowed to impact when the retainer plug became loose during previous shots in the series. An examination of the transducer revealed one of the strain gages with

its bonding epoxy and encapsulant to be completely separated from the column.

3.1.6 On-Structure Tests. Several tests were made with Gage IF-1-WES mounted flush in a rigid concrete base in the SBLG (Figure 3.10). Several depths of sand cover were placed over the mounted gage for testing. This arrangement approximated the design condition of flush mounting in a very rigid (relatively unyielding) structure at a soil (sand in this case) interface. The test specimen was loaded statically by fluid pressure transmitted through a rubberized membrane.

The static response of Gage IF-1-WES under this test condition is shown in Figure 3.11. It can be seen from this figure that the gage does, in fact, indicate higher than applied pressures, and at an essentially constant level at loadings above 100 psi. These data support the basic design hypothesis. Tests on stiff, free-field soil stress transducers, reported in Reference 10, yielded similar data.

Several dynamic tests were made under the same test conditions as the static tests. Pressure histories (Figure 3.12) were "clean," showing very little noise. Signal rise times ranged from 0.2 to 0.4 msec. The oscillations appearing on the record are characteristic of the test chamber and not of the gage itself. (This phenomenon is discussed briefly in Reference 10.)

3.2 FS GAGE

A smaller gage was needed for use on model structures and, since preliminary results with the IF gages were promising, a smaller transducer was designed using the same principles. This gage, designated FS-1, was made of aluminum and was designed for higher strain levels so that conventional foil strain gages could be used. This requirement led to a rectangular (rather than square) cross section in the load column. Figures 3.13 and 3.14 show construction details.

This gage was originally designed to be cast into the model structure in order to reduce weight of mounting flanges, etc. Figure 3.15 shows the gage mounted in a cylinder of "sandcrete," a sand-fiber glass resin mixture. All tests of this gage were made in this mount. Later versions of this gage had threaded housings.

Design calculations embraced the same equations as those for the IF gage (Section 2.2) and are not repeated here. A listing of gage characteristics is given in Table 3.1.

The effects of environmental temperature changes on gage output were investigated and found to be insignificant, amounting to approximately 0.374 $\mu\epsilon/^{o}F$. This was, primarily, the result of the low thermal sensitivity of the foil strain gages and the close electrical balance achieved in the circuit.

Mechanical loading of the cell face produced a linear response

up to 12,000 pounds applied force. Static calibration tests were conducted up to 500 psi in the SBLG with Gage FS-1 buried in dense, dry Cook's Bayou No. 1 sand at depths of cover of 1/2, 1, 3-1/2, and 16 inches. In addition to the static tests, two dynamic tests (nominally at 100 and 200 psi) were made at the 16-inch depth of burial. A plot of the applied versus measured pressures is shown as Figure 3.16. The data are from the third loading cycle since slopes shifted with each cycle up to the third. After the third cycle, the specimens had stabilized and little change was noted in measurements taken between the third and sixth loading cycles.

Static stresses were greater than the surface load by approximately 1 percent at the 1/2-inch depth, 8 percent at 1 inch, and 6 percent at 3-1/2 inches. The measured stress at the 16-inch depth was 24 percent less than the surface load. This value was common for both the static and dynamic conditions.

A plot of normalized stress (ratio of measured stress P_m at depth to the applied surface pressure P_{so}) with depth (Figure 3.17) shows the stress falloff to the 16-inch depth as well as sidewall friction effects in the test chamber. The sidewall friction curve was mathematically constructed from equations developed in Reference 11. The low stress recorded at the 16-inch level was probably due to sidewall friction.

3.3 M-1 GAGE

An airblast gage design came as a logical extension of the structure-interaction gage development, since satisfactory results were obtained from airblast measurements made with IF-5-KB mounted in the firing tube of the SBLG (Section 3.1.5). The major differences from the stress gage design are increased column deflection and a cross-section change from square to rectangular similar to the FS-1 design. The structural elements were fabricated from type 416 stainless steel. A drawing of the gage is shown as Figure 3.18. Figure 3.19 shows the complete transducer with cable connector attached.

Because of the relatively low strain levels expected to develop, solid-state strain gages were employed in the same manner as in the IF gage. The strain gages selected for this transducer were P-type silicon similar to those used in Gage IF-1-WES. The gage factor for this lot was 52.1 with a resistance of 117.9 ± 1.7 ohms. It was felt that with the lower gage factor (about one-half that of the gages used on IF-1-WES), the accompanying thermal sensitivity would be reduced comparably. This assumption was borne out in testing.

The design pressure limit of 500 psig was chosen as a practical limit with allowance for 100 percent overload without damage to the gage. The design calculations followed the same method as for the

two previous gage types (Section 2.2). Gage characteristics are listed in Table 3.1.

Tests were made to determine gage response both statically and dynamically. Static pressure calibrations up to 500 psig showed the gage to be linear for this range.

Dynamic tests were made with the gage mounted in the shock tube end plate as shown in Figure 3.20. A step pulse air shock was applied in each test.

With hard-mounting (metal-to-metal) the gage was extremely acceleration-sensitive (Figure 3.20a). Additional tests were made to determine the effectiveness of shock-mounting and the relative contributions of pressure and acceleration on the gage output.

Figure 3.20b shows the hard-mounted gage to be very acceleration-sensitive; in this test the pressure was isolated from the gage face with a small plate. A cast silicone rubber shock mount virtually eliminated the acceleration signal when the shock wave was not allowed to strike the gage face (Figure 3.20c). Figure 3.20d shows an acceptable pressure measurement made using the rubber mount. These tests clearly demonstrate the importance of shock-mounting in severe acceleration environments.

Teflon and nylon proved to be quite satisfactory as shock-mounting materials in later tests. Both materials have the advantage

over silicone rubber in rigidity and strength, and are recommended for use with the OSS gage.

TABLE 3.1 OSS GAGE CHARACTERISTICS

Gage	Output Full Scale	Linearity Full Scale		Hysteresis		Strain Sensitivity	Thermal Sensitivity	Maximum Usable Range
		+70 F	+120 F	+70 F	+120 F			
	mv/v	pct	pct	pct	pct	$\mu\epsilon$/psi	10^{-2} $\mu\epsilon/psi/^{o}F$	10^3 psi
IF-1-WES	2.57	$\pm$1.68	$\pm$0.91	$\pm$4.01	$\pm$3.60	10	0.73	20
IF-2-BLH	2.57	$\pm$0.63	$\pm$0.27	$\pm$2.54	$\pm$1.08	6	1.44	20
IF-5-KB	1.07	$\pm$1.02	$\pm$0.56	$\pm$2.04	$\pm$0.38	4	0.44	20
IF-6-MSI	2.08	$\pm$1.53	a	$\pm$1.28	a	8	0.26	20
FS-1	0.81	$\pm$0.45	$\pm$0.45	$\pm$0.80	$\pm$0.80	3	0.07	2
M-1	2.51	$\pm$0.89	$\pm$3.96	$\pm$3.57	$\pm$14.78	10	3.21	1

[a] Gage became defective.

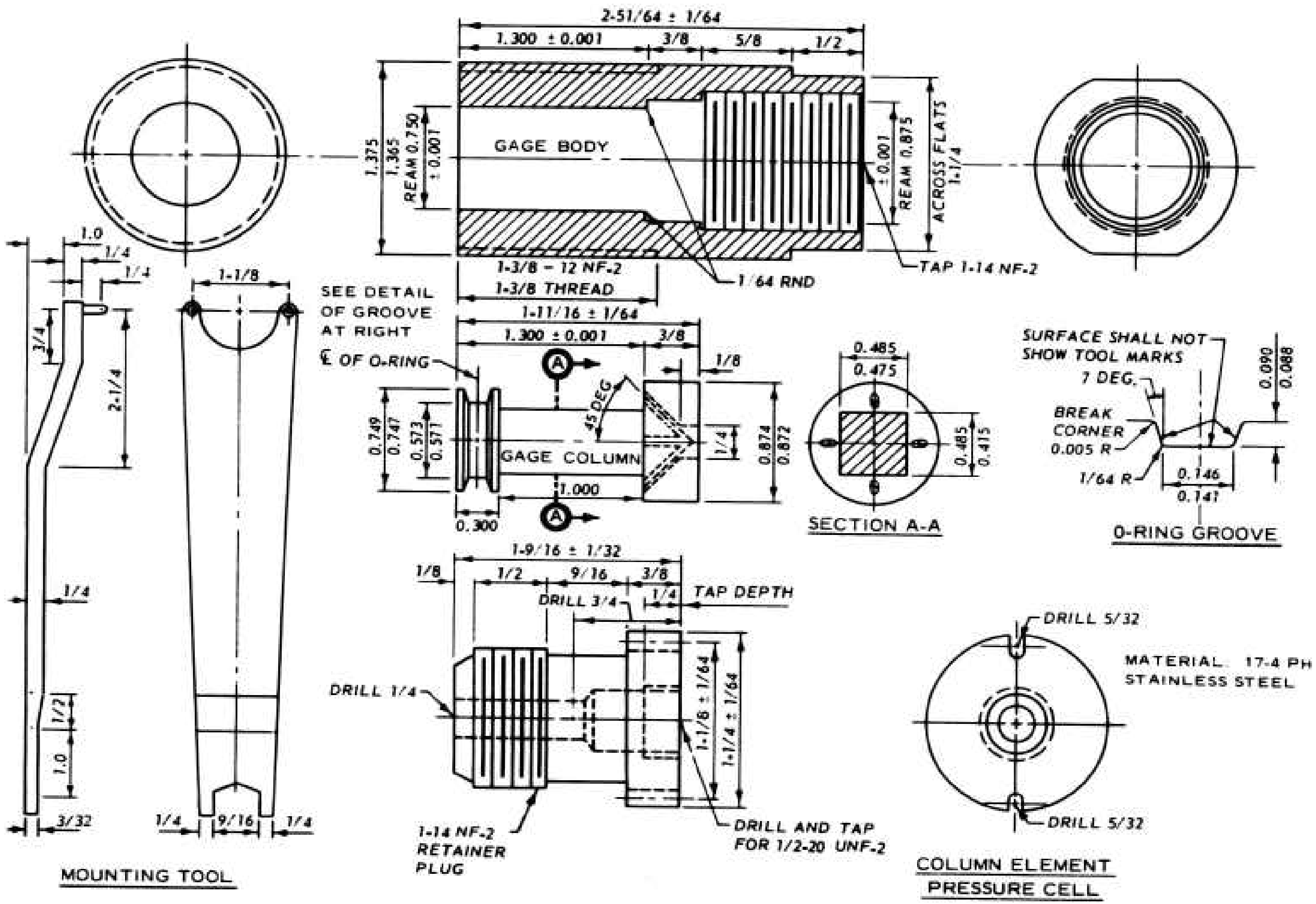

Figure 3.1 Drawing of IF gage. Dimensions are in inches.

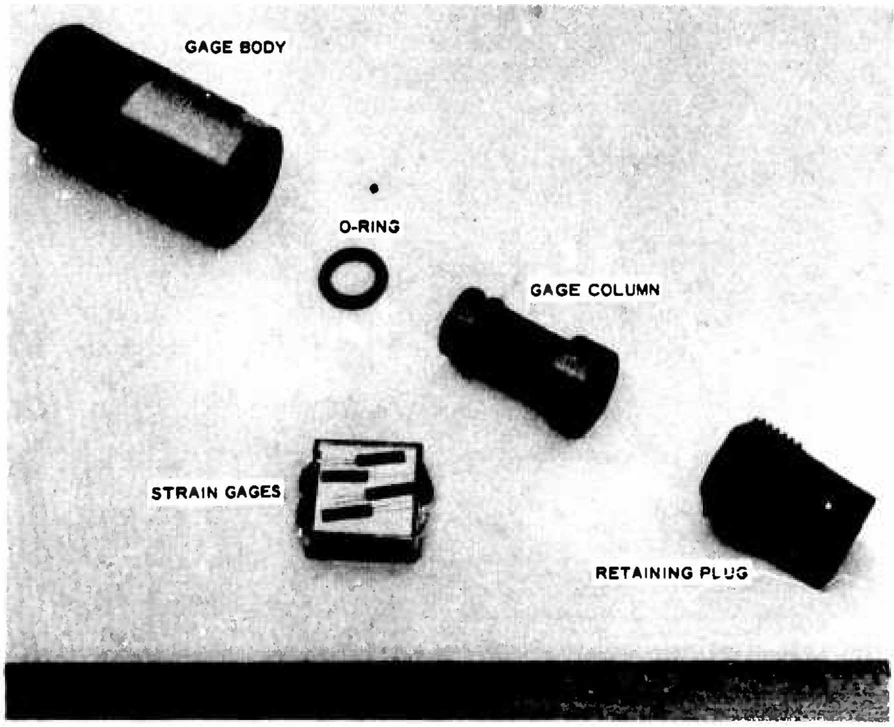

a.
Unassembled

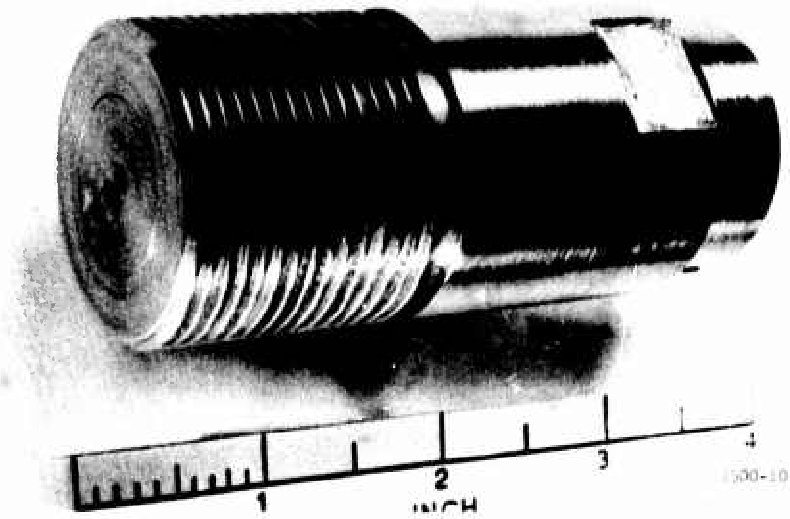

b.
Assembled

Figure 3.2 IF gage assembly.

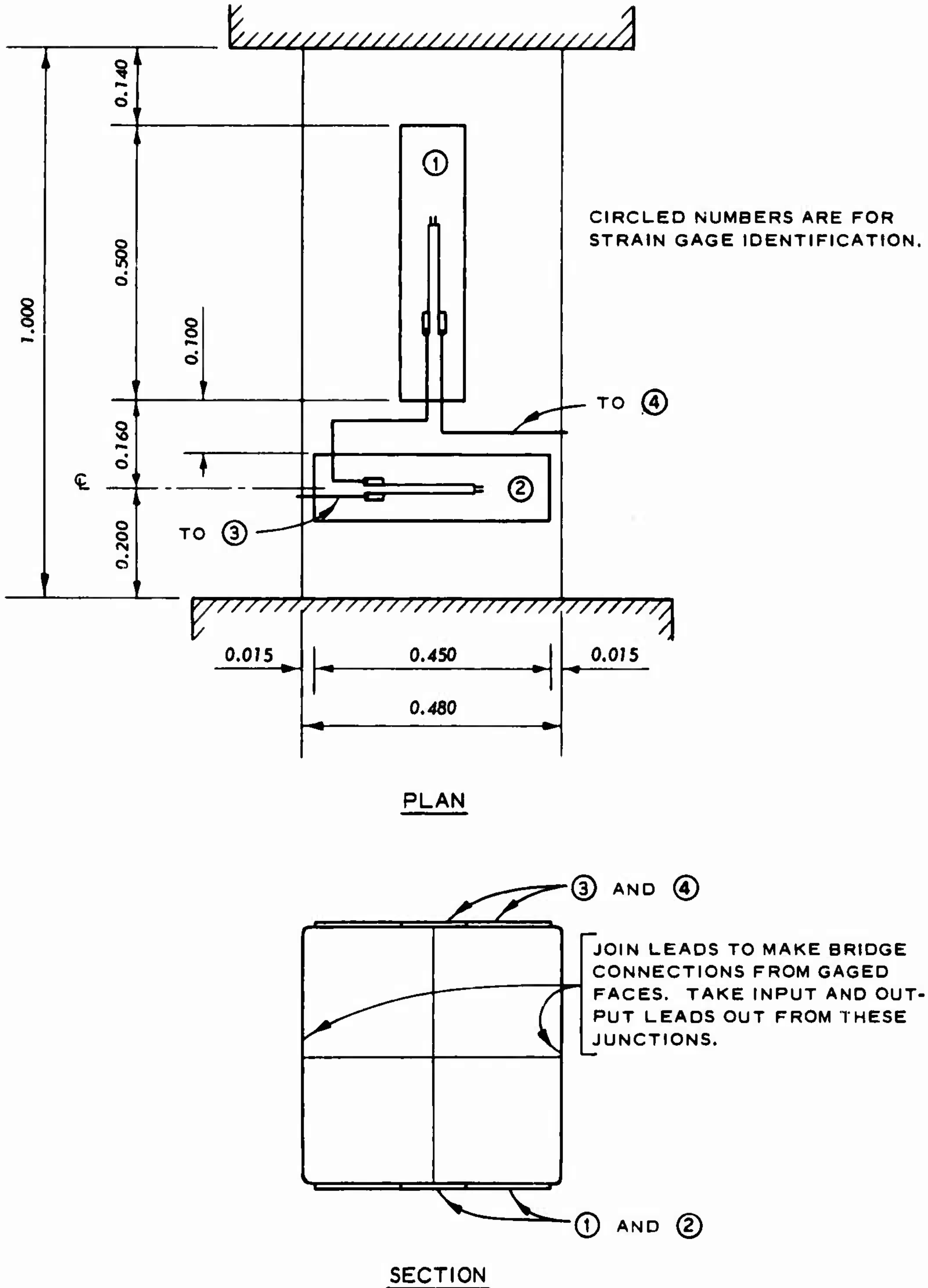

Figure 3.3 Strain gage placement for IF gage. Dimensions are in inches.

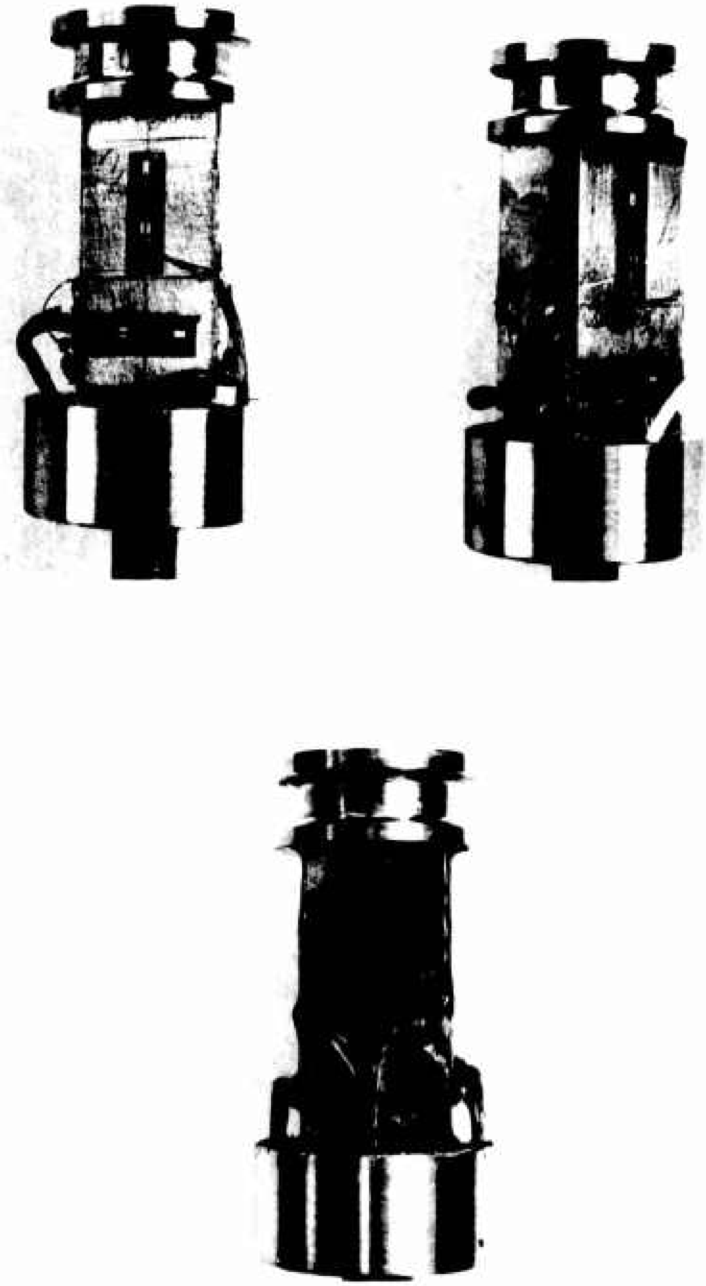

Figure 3.4 Strain gages mounted on load column of IF gage.

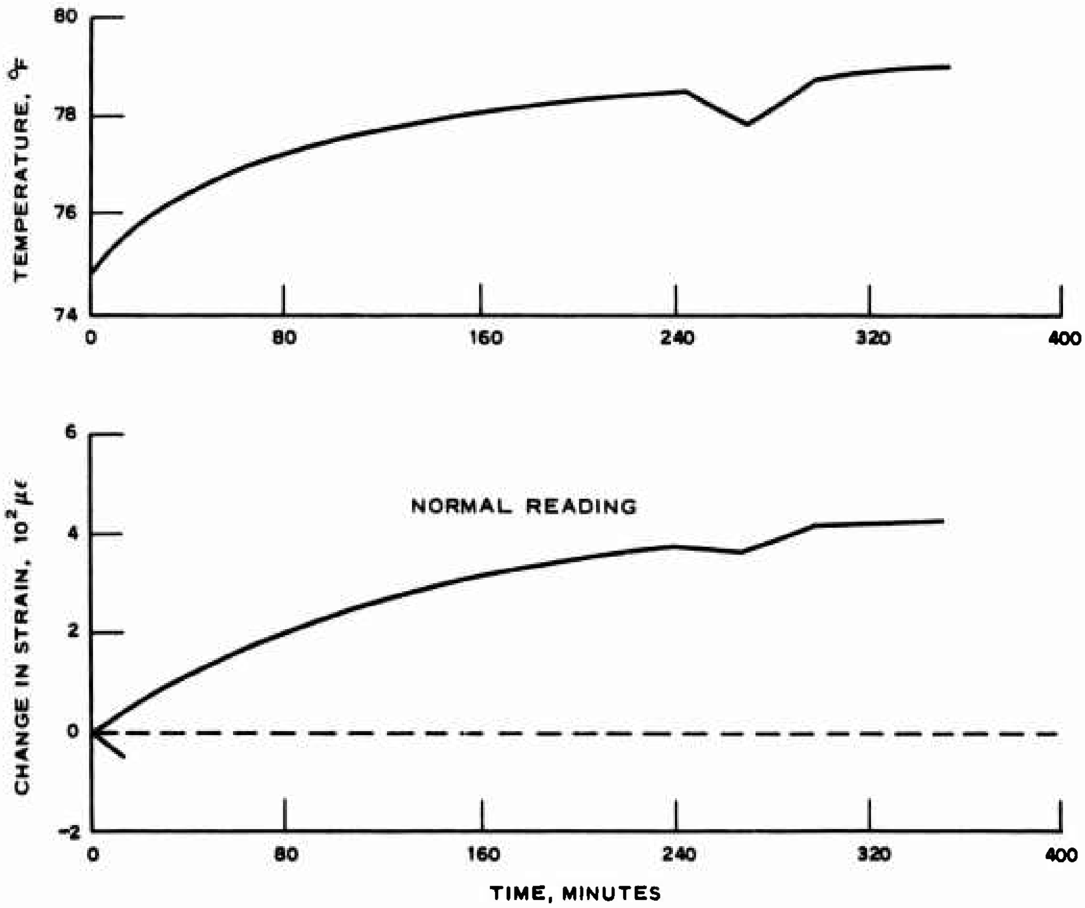

Figure 3.5 Thermal zero drift, Gage IF-1-WES.

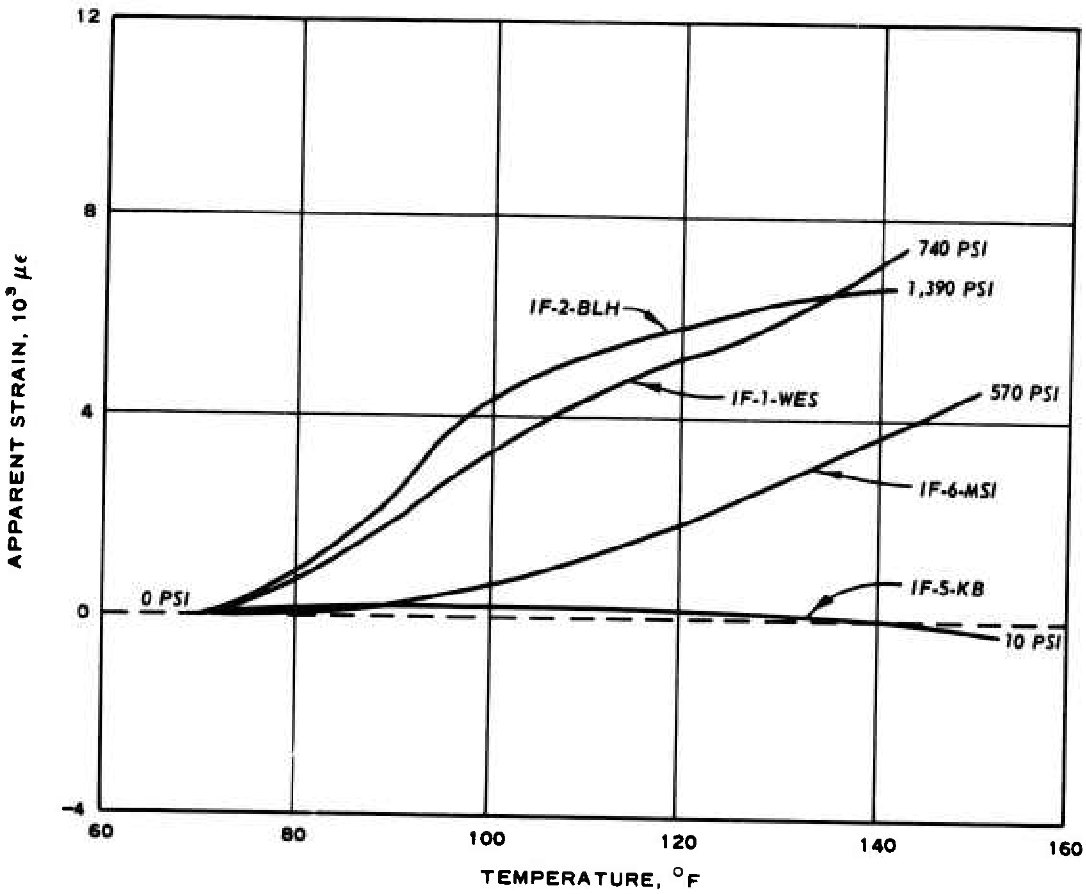

Figure 3.6 Thermal zero drift, all IF gages.

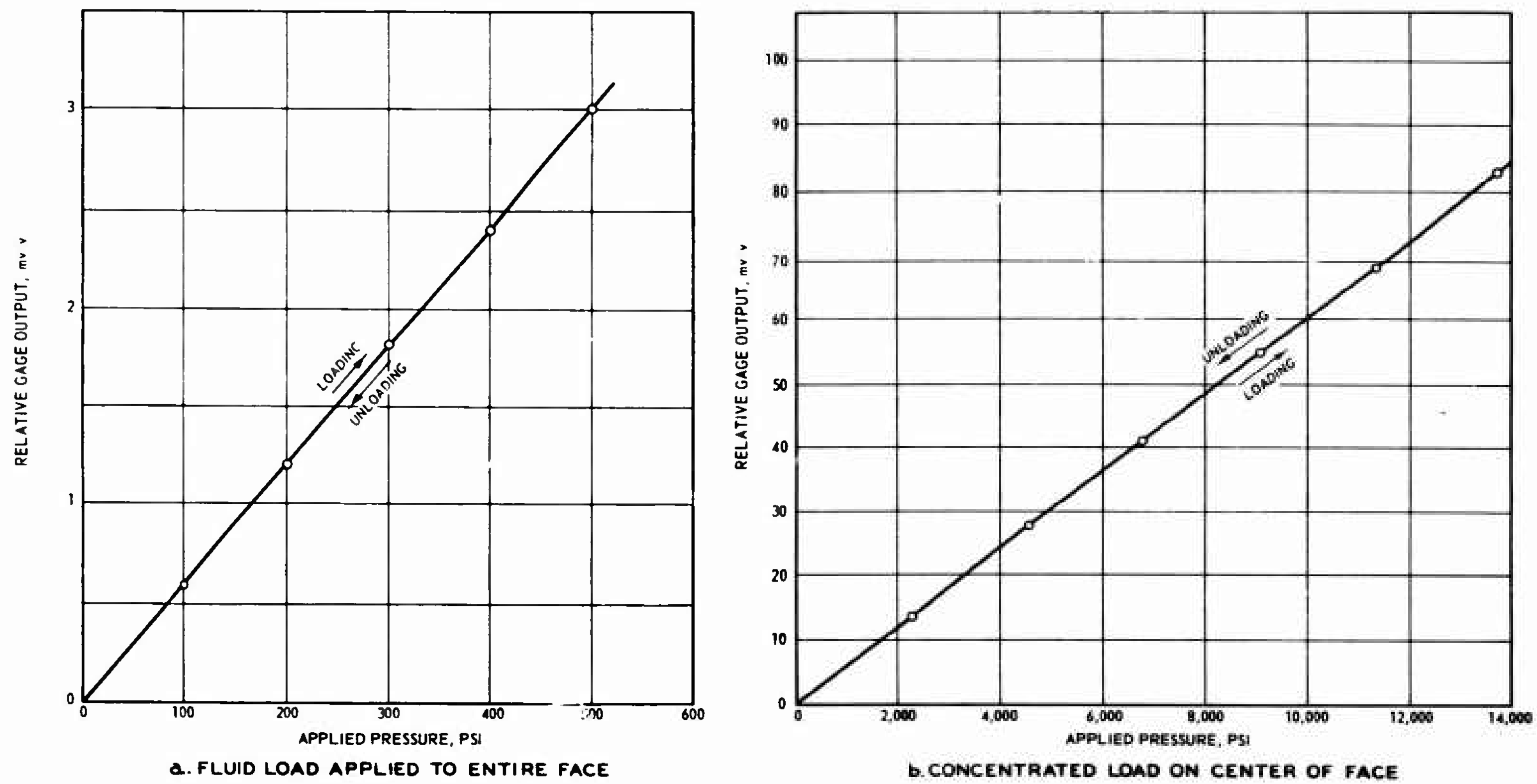

Figure 3.7 Calibration 1, gage sensitivity, IF gage.

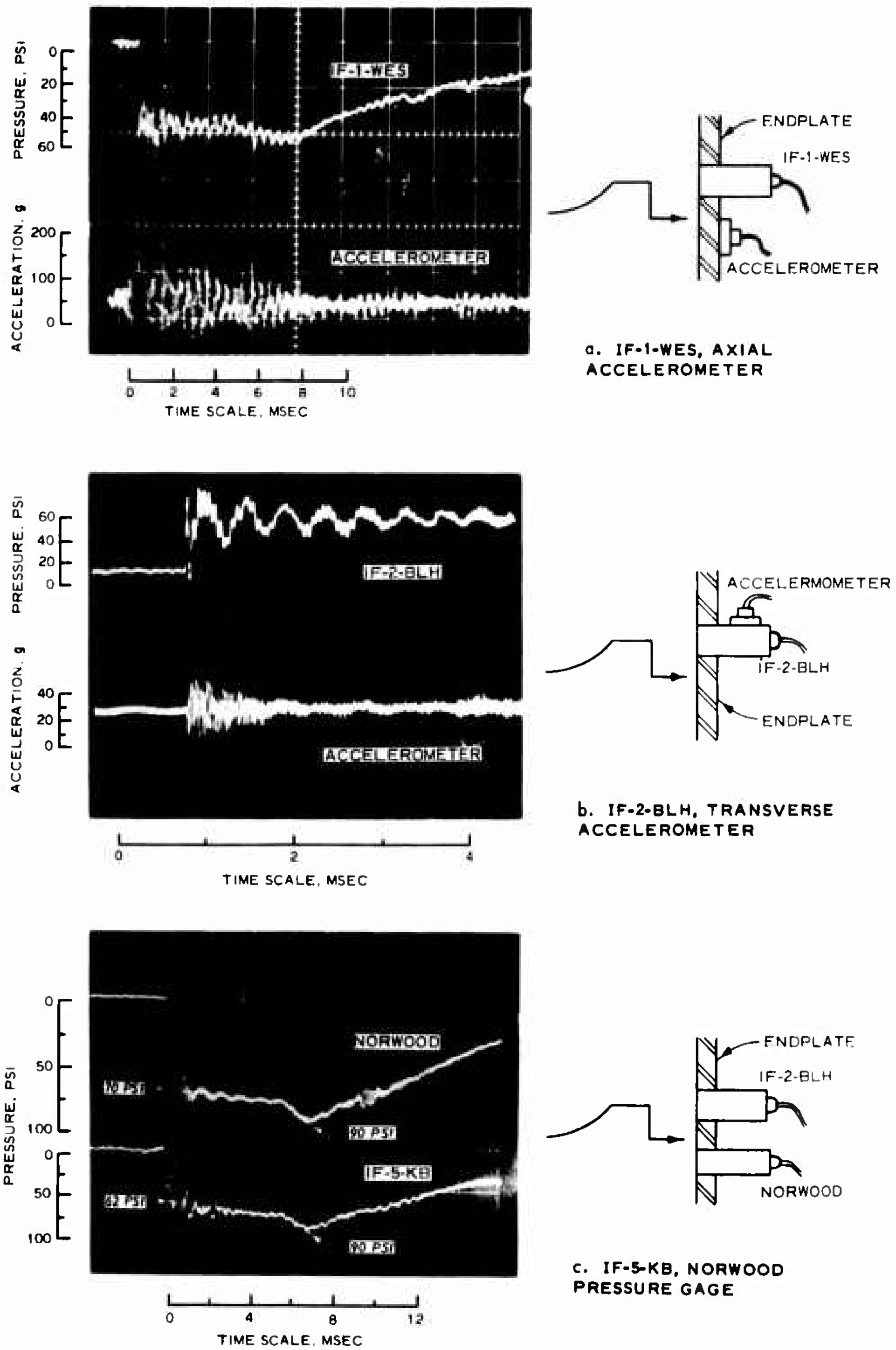

Figure 3.8 Response of IF gages to air-shock loading.

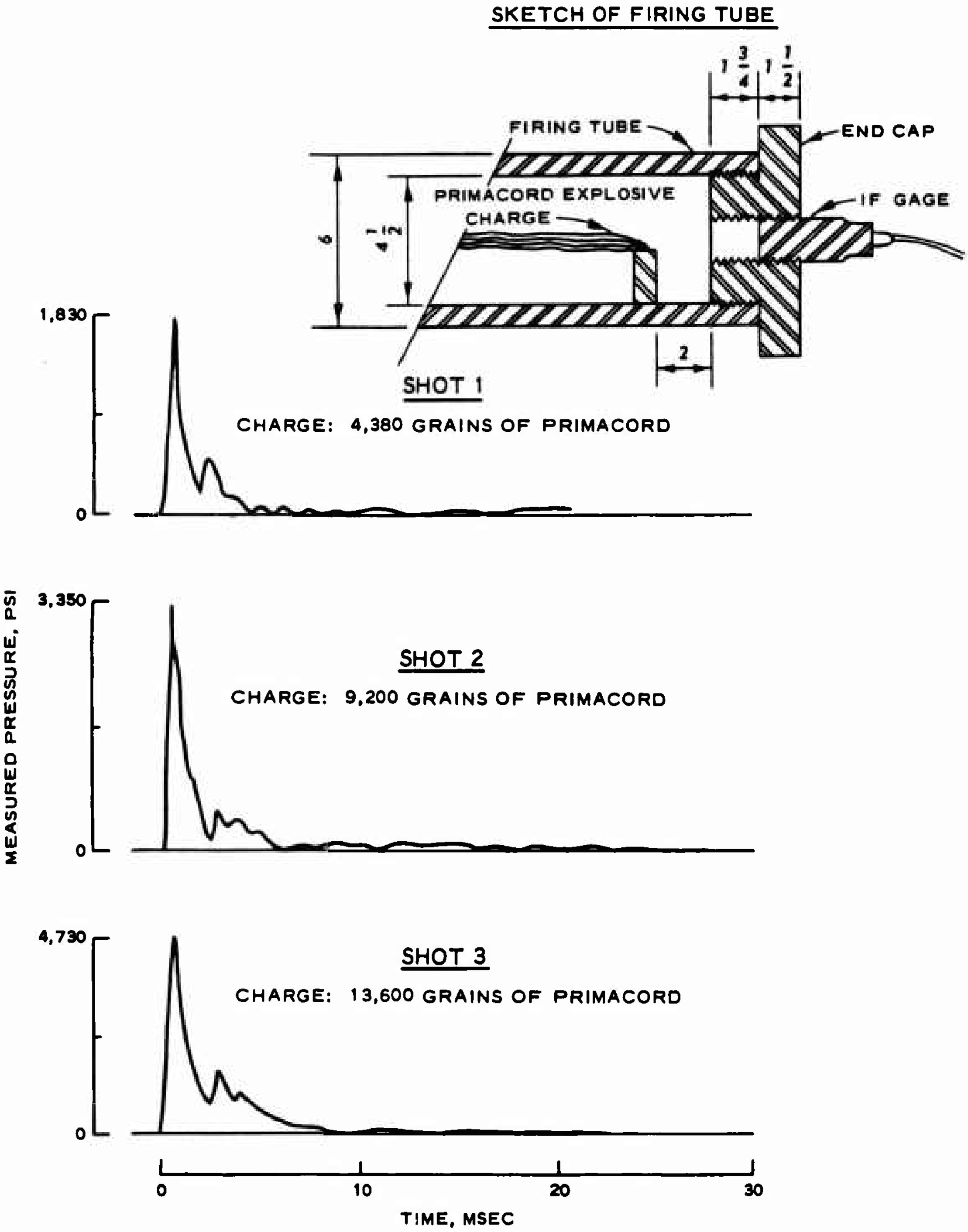

Figure 3.9 IF gage firing tube pressure measurements. Firing tube dimensions are in inches.

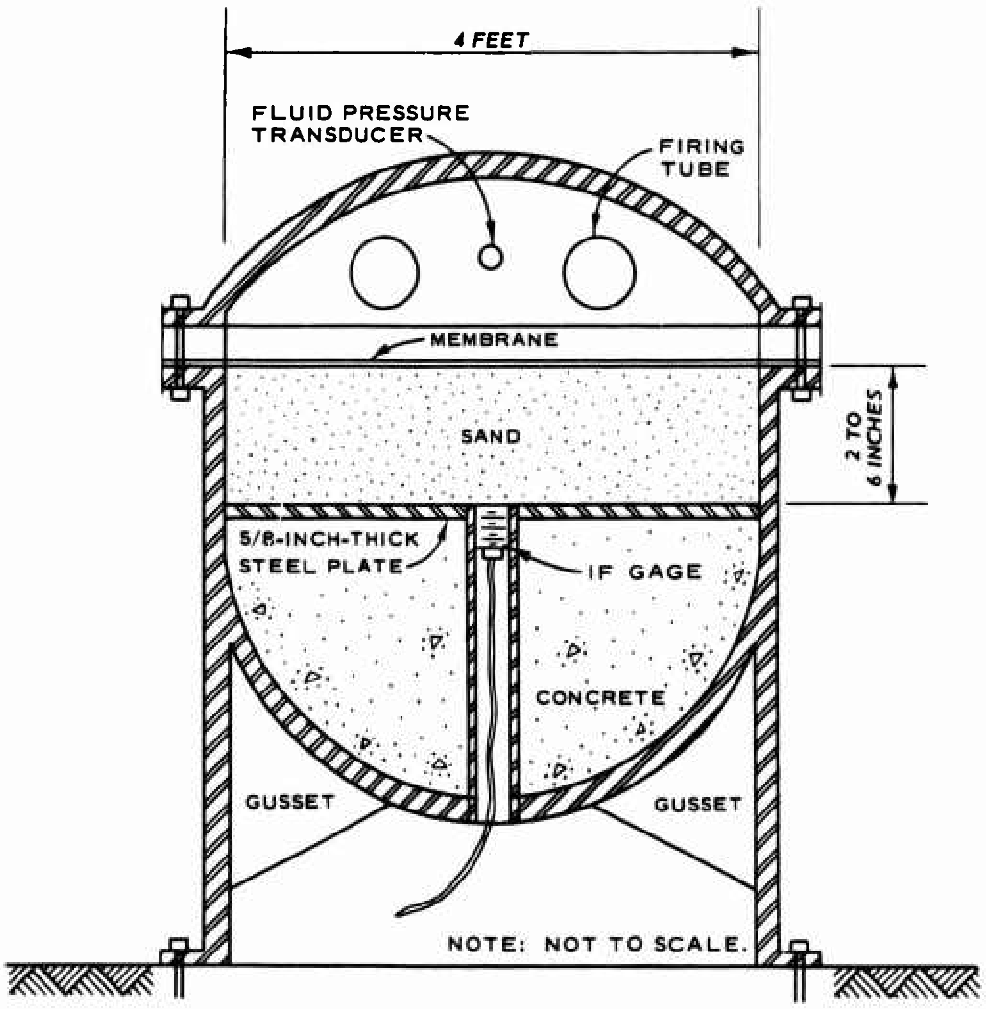

Figure 3.10 Gage IF-1-WES mounted in concrete base in SBLG for testing.

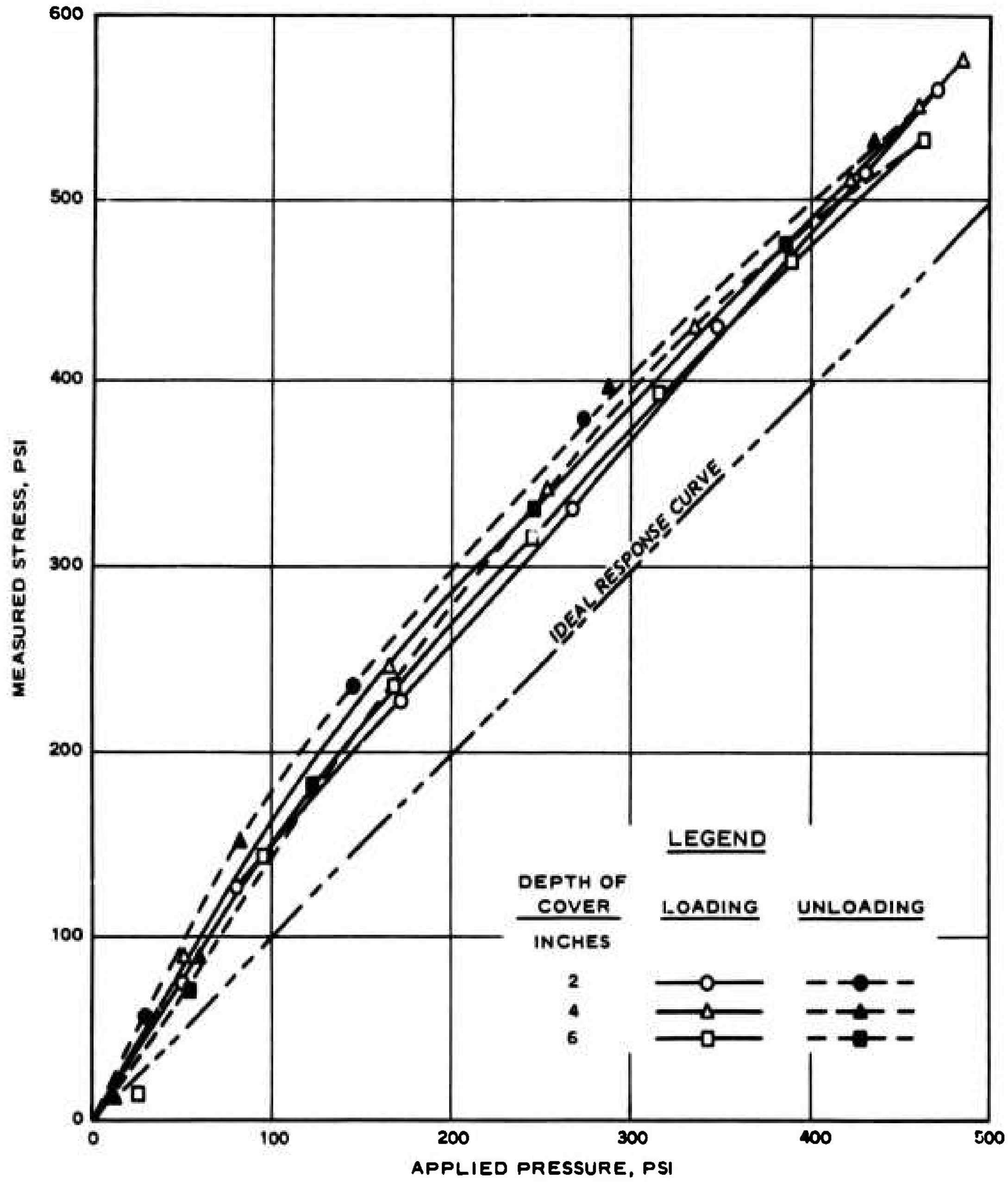

Figure 3.11 Static response of Gage IF-1-WES flush-mounted in a rigid structure in dry sand.

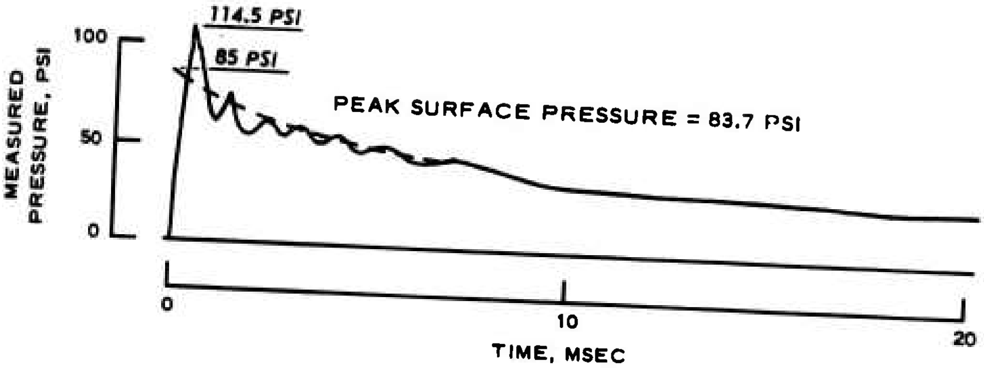

Figure 3.12 Dynamic pressure-time signature, Gage IF-1-WES flush-mounted in rigid structure under 2-foot sand cover.

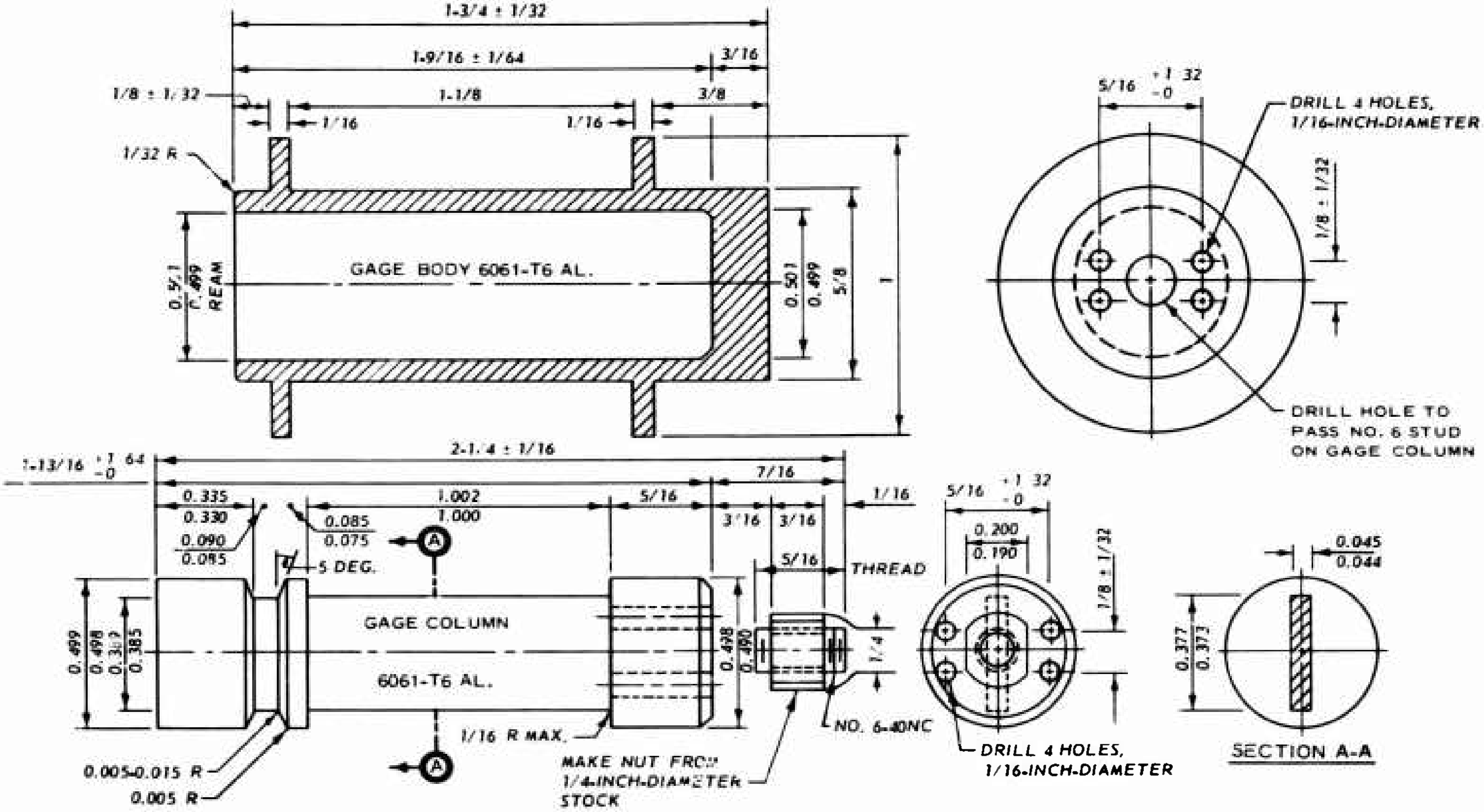

Figure 3.13 Drawing of Gage FS-1. Dimensions are in inches.

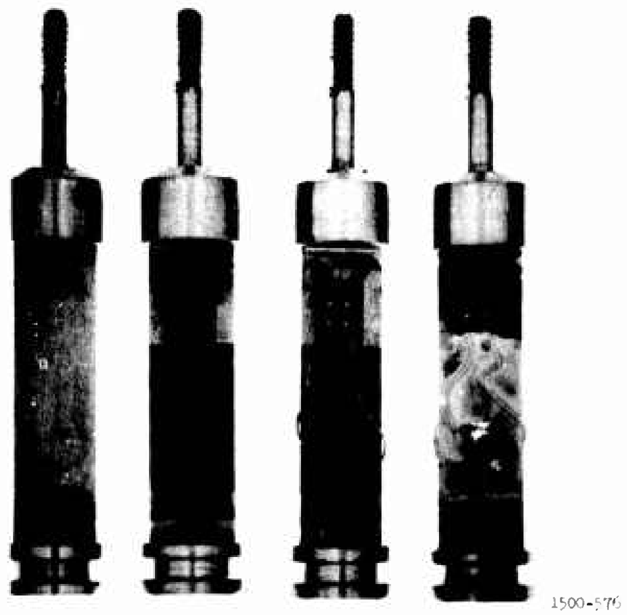

a. Stress gage attachment on load column.

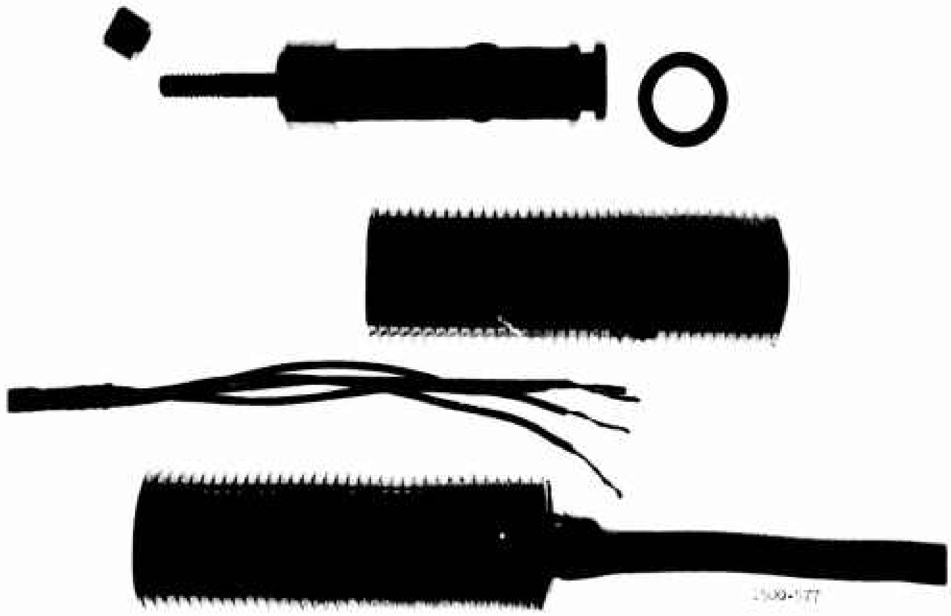

b. Gage components and assembled gage.

Figure 3.14 FS gage assembly.

Figure 3.15 Gage FS-1 mounted in "sandcrete" cylinder (pseudostructure).

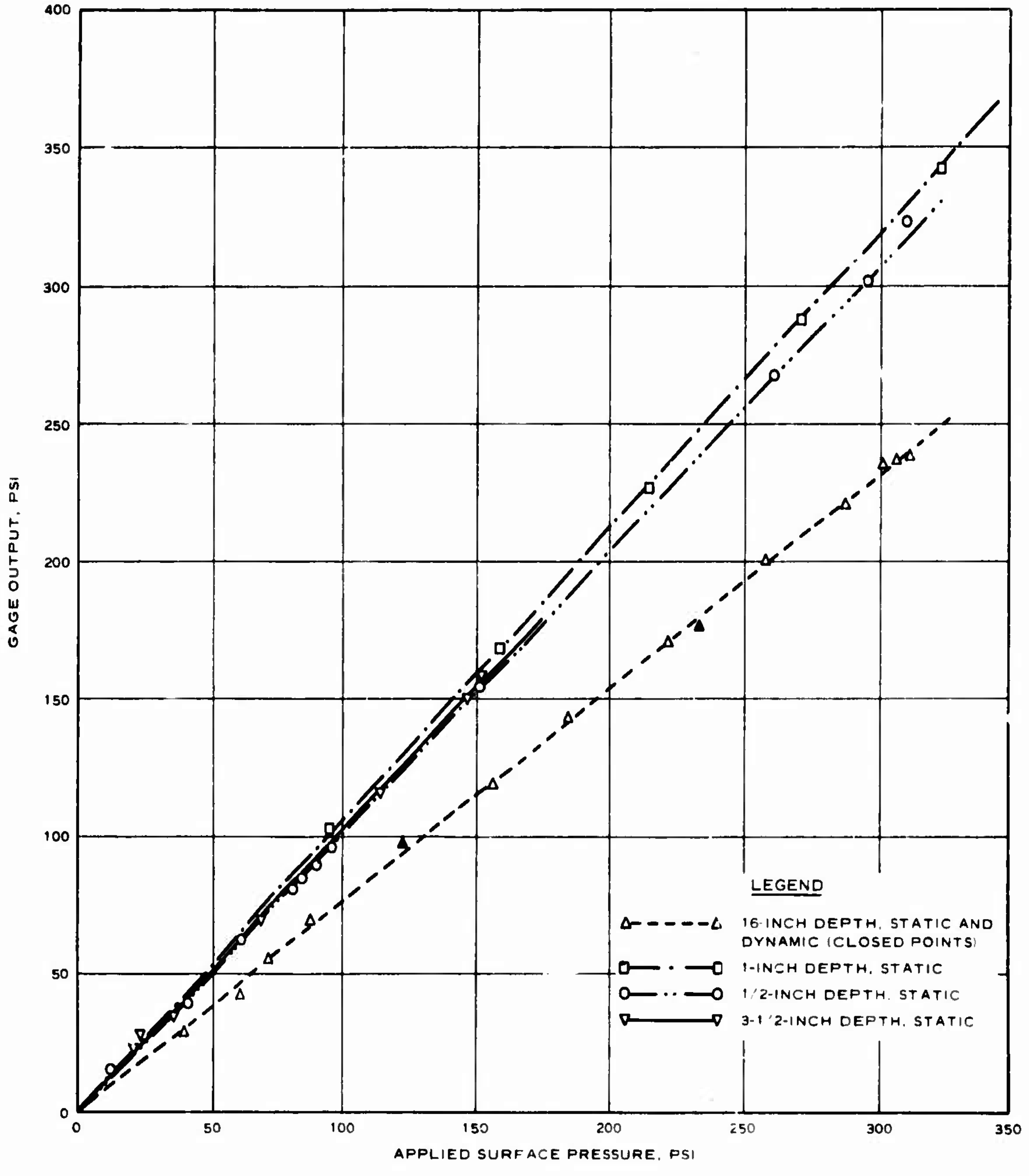

Figure 3.16 Response of Gage FS-1 in dry sand.

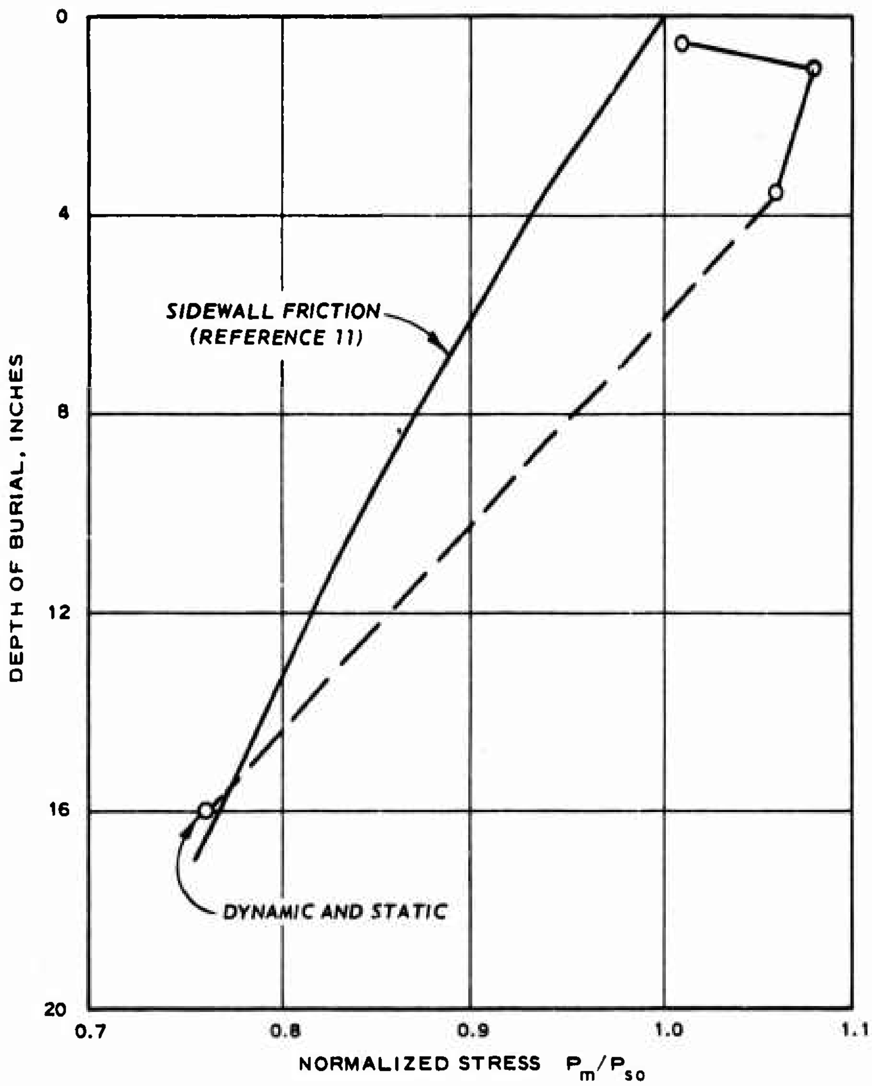

Figure 3.17 Stress attenuation with depth in sand, Gage FS-1.

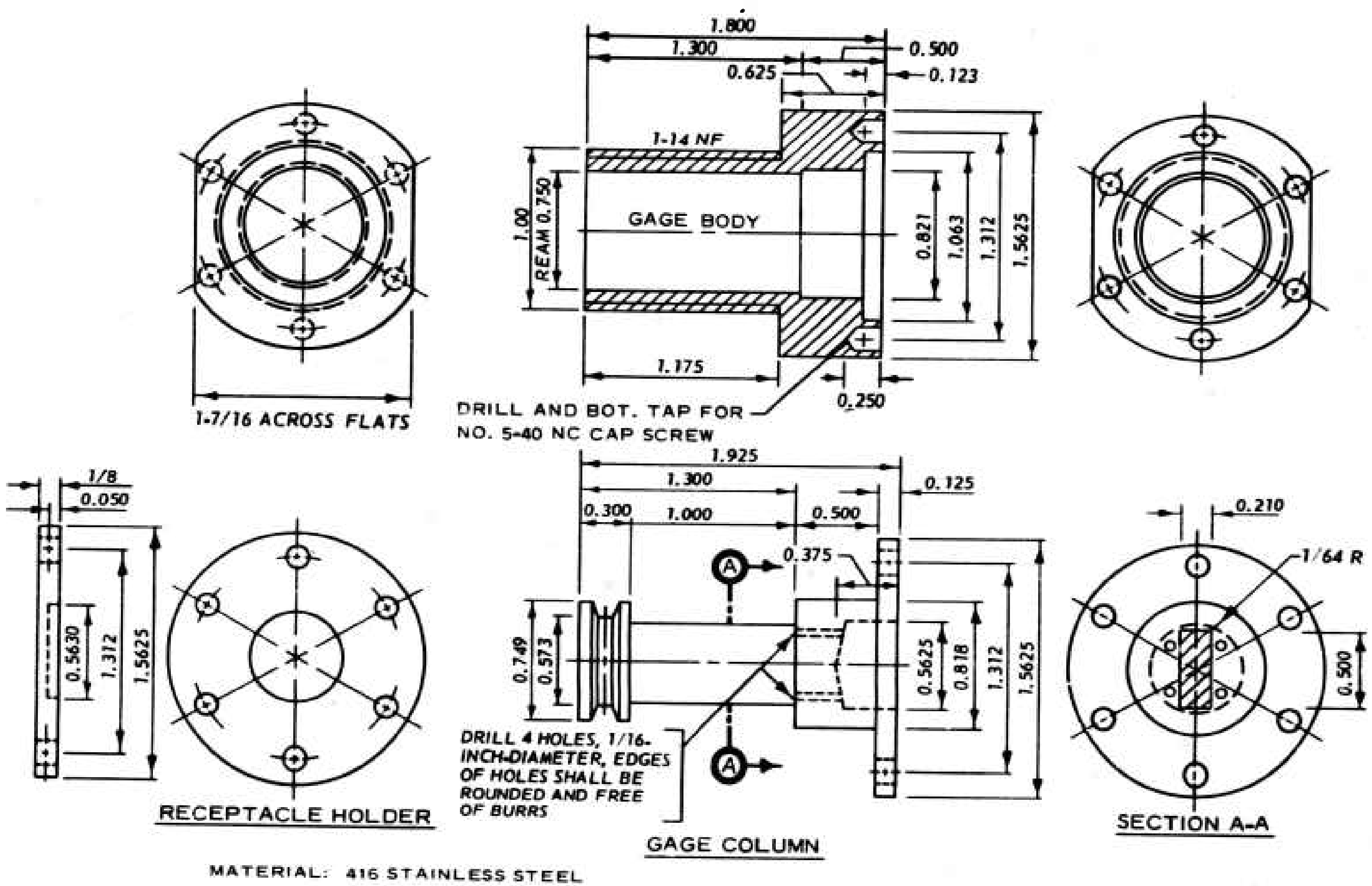

Figure 3.18 Drawing of M-1 gage. Dimensions are in inches.

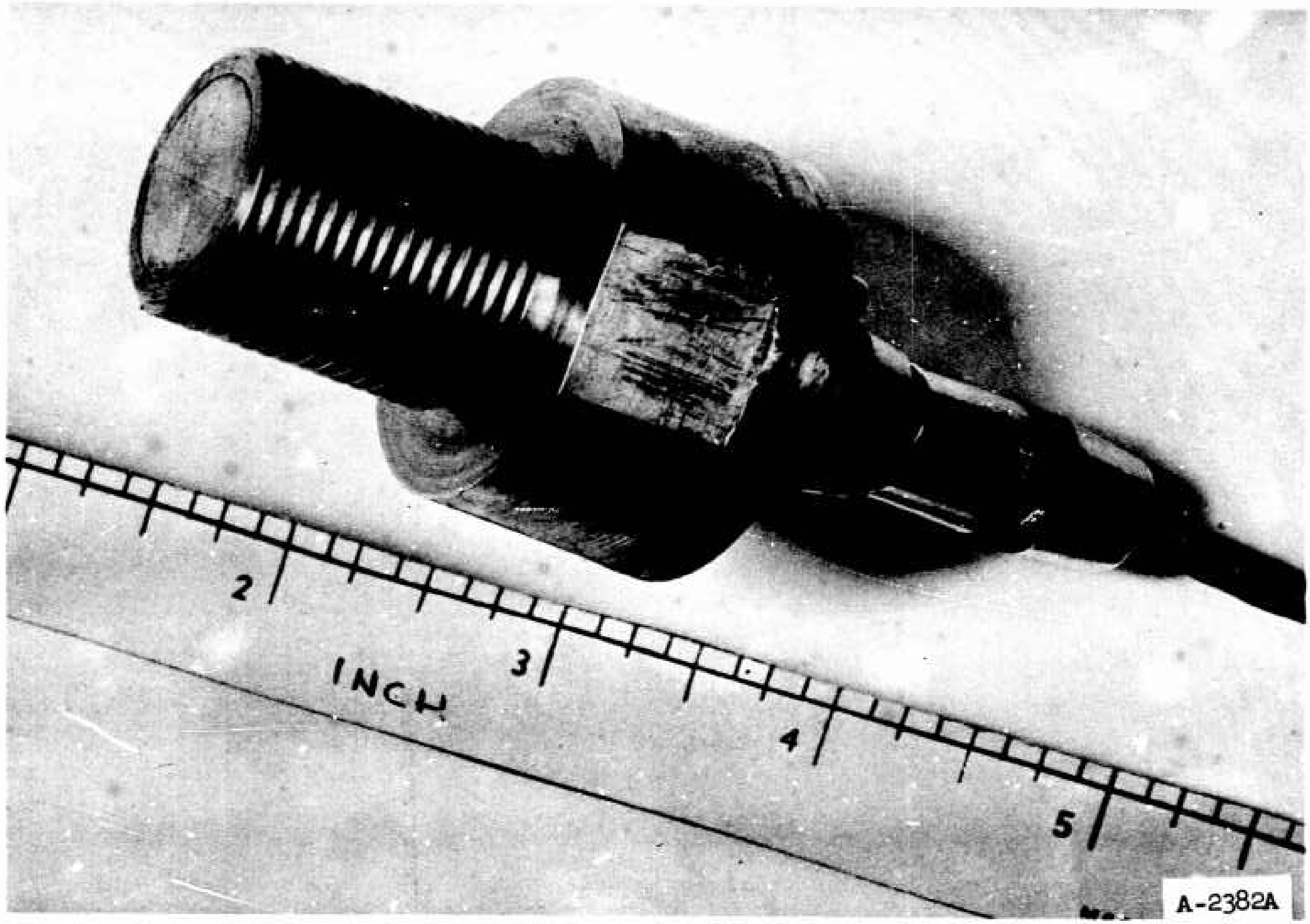

Figure 3.19 M-1 gage assembled.

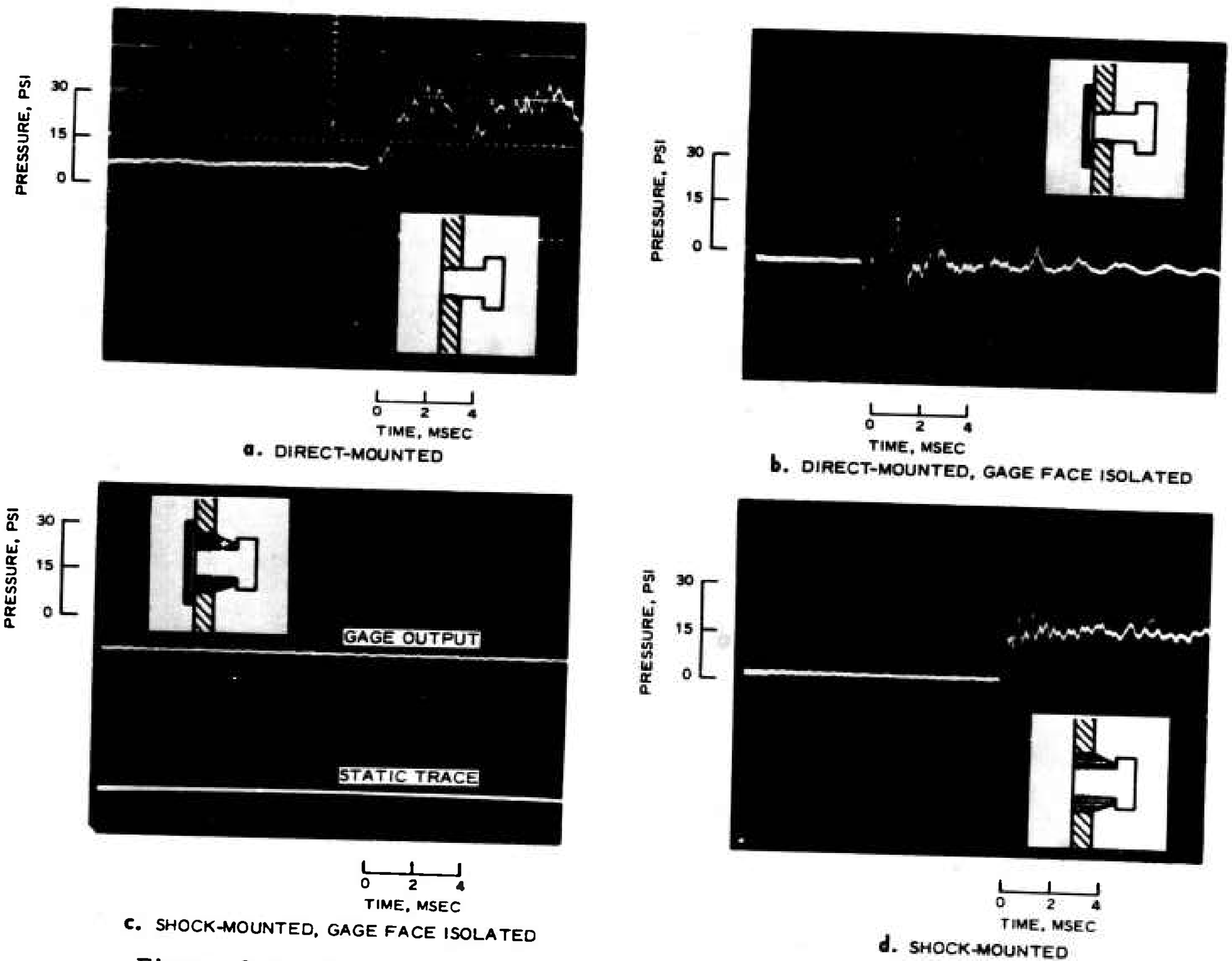

Figure 3.20 M-1 gage response for different mounting conditions.

CHAPTER 4

CONCLUSIONS AND RECOMMENDATIONS

The basic principles of the family of gages developed in this research have been demonstrated to be sound. Simple, reliable, linear, rugged transducers can be made using the end-loaded piston design. It was also determined that these gages may be used for measuring airblast pressure as well as soil pressure. The end-loaded piston design has several advantages over thin, diaphragm-type gages which are normally available commercially for airblast measurement. The column element deforms linearly and, due to its stiffness, is usable over a great range of pressures when instrumented with sensitive piezoresistive sensors. The mass of material in the column acts as an excellent heat sink and allows considerable pressure-time resolution before transient thermal effects are imposed on the gage output. The IF gages were used with excellent results to measure pressure levels of approximately 5,000 psi inside the firing tubes (detonation chambers) of the blast generator. Such measurements are difficult to make because of attendant heat and acceleration which tend to obscure the pressure information. The one commercial, high-pressure airblast gage available for testing (claimed to be usable up to 60,000 psi) failed completely at less than 5,000 psi. A comparably placed IF gage produced a satisfactory output in the same test.

Because of the gages' stiffness, overregistration occurs when measurements are made in soils. It should be pointed out that the gage registration, however, is not a simple function of moduli ratios, but is affected to large extent by structure and medium placement. In this light, it remains for the structural designer to consider carefully the gage mount as well as the transducer itself that will meet the requirements that the gage deform equally with the surrounding structure (for flush mounting), and that proper coupling is achieved between the structure (or structural element) and the medium. The IF gage was found to overregister statically by about 25 percent when mounted in a stiff steel plate under sand cover.

The FS gage has proven satisfactory for use in thinner walled structures (model structures). It is basically a miniaturized version of the IF gage. Overregistration for the FS gages is less than that for the IF gage due to the higher compliance of the FS gages. Maximum overregistration is about 10 percent for very shallow soil cover, and there is essentially no overregistration for the gage mounted on deeply buried, concrete-like structures.

The IF gage and FS gage can be used interchangeably. The controlling factors are size and mass allowable and environmental pressure level. IF gages may be used on large, stiff structures subjected to surface pressures up to 20,000 psi or in high fluid

pressure environments such as firing tubes or detonation chambers. FS gages are recommended for use on thinner walled, more compliant structures at lower test pressures (2,000 psi or less).

The M-1 airblast gage can be used as a structure or fluid pressure gage, but is limited to pressures under 1,000 psi. Capacity of this (and other) designs can be increased by enlarging the area of the load column.

Additional research is recommended to evaluate the gage performance more completely in static and dynamic soil tests. A range of soil types from coarse dry sand to moist fat clays should be investigated. Future research on gages for measuring soil pressures on structures should be concentrated on development of small gages for use with models and thin-walled structures. An additional requirement exists for reliable methods of emplacing such gages from within the structure when access to the exterior is prohibited by backfill or native soil.

REFERENCES

1. B. Chan; "Design of a Transducer for Pressure Measurements on Buried Concrete Structures"; Miscellaneous Paper No. 1-593, August 1963; U. S. Army Engineer Waterways Experiment Station, CE, Vicksburg, Mississippi; Unclassified.

2. A. C. Wiffin and S. A. H. Morris; "Piezoelectric Gauge for Measuring Dynamic Stresses Under Roads"; The Engineer, 27 April 1962, Vol. 213, No. 5544, Pages 741-746; Morgan Brothers Ltd., London, England; Unclassified.

3. D. W. Taylor; "Review of Pressure Distribution Theories, Earth Pressure Cell Investigations and Pressure Distribution Data"; Soil Mechanics Fact Finding Survey, Progress Report, April 1947, Pages 179-332; U. S. Army Engineer Waterways Experiment Station, CE, Vicksburg, Mississippi; Unclassified.

4. G. E. Monfore; "An Analysis of the Stress Distributions in and near Stress Gages Embedded in Elastic Solids"; Structural Research Laboratory Report No. SP-26, June 1950; U. S. Department of the Interior, Bureau of Reclamation, Research and Geology Division, Denver, Colorado; Unclassified.

5. K. R. Peattie and R. W. Sparrow; "The Fundamental Action of

Earth Pressure Cells"; Journal of the Mechanics and Physics of Solids, April 1954, Vol. 2, No. 3, Pages 141-155; Pergamon Press, Inc., New York, New York; Unclassified.

6. D. H. Trollope and D. T. Currie; "Small Embedded Earth Pressure Cells--Their Design and Calibration"; Proceedings of the Third Australia-New Zealand Conference on Soil Mechanics and Foundation Engineering, 22-26 August 1960, Pages 145-151; University of Sydney, N. S. W., Australia; Unclassified.

7. J. Boussinesq; "Application des Potentiels; a l'Etude de l'Equilibre et du Mouvement des Solides Elastiques"; 1885; Gauthier-Villars, Paris, France; Unclassified.

8. J. R. Hossley; "Small Blast Load Generator Tests Using M-9 Propellant"; Miscellaneous Paper No. 1-913, August 1967; U. S. Army Engineer Waterways Experiment Station, CE, Vicksburg, Mississippi; Unclassified.

9. G. E. Albritton; "Description, Proof Test, and Evaluation of Blast Load Generator Facility"; Technical Report No. 1-707, December 1965; U. S. Army Engineer Waterways Experiment Station, CE, Vicksburg, Mississippi; Unclassified.

10. J. K. Ingram; "Development of a Free-Field Soil Stress Gage for Static and Dynamic Measurements"; U. S. Army Engineer Waterways Experiment Station, CE, Vicksburg, Mississippi; In preparation; Unclassified.

11. J. V. Zaccor and others; "Study of the Dynamic Stress-Strain and Wave Propagation Characteristics of Soils; Concepts of Shock Behavior in a Granular Medium"; WES Contract Report No. 3-91, Report 4, March 1965; United Research Services, Inc., Burlingame, California; Unclassified.

Unclassified

Security Classification

DOCUMENT CONTROL DATA - R & D		
(Security classification of title, body of abstract and indexing annotation must be entered when the overall report is classified)		
1. ORIGINATING ACTIVITY (Corporate author) U. S. Army Engineer Waterways Experiment Station Vicksburg, Mississippi	2a. REPORT SECURITY CLASSIFICATION Unclassified	
	2b. GROUP	
3. REPORT TITLE DEVELOPMENT OF ON-STRUCTURE STRESS GAGES		
4. DESCRIPTIVE NOTES (Type of report and inclusive dates) Final report		
5. AUTHOR(S) (First name, middle initial, last name) Russell W. Faust James K. Ingram		
6. REPORT DATE November 1967	7a. TOTAL NO. OF PAGES 85	7b. NO. OF REFS 11
8a. CONTRACT OR GRANT NO.	9a. ORIGINATOR'S REPORT NUMBER(S) Technical Report No. 1-801	
b. PROJECT NO.		
c. NWET Subtask 11x13x03	9b. OTHER REPORT NO(S) (Any other numbers that may be assigned this report)	
d.		
10. DISTRIBUTION STATEMENT This document has been approved for public release and sale; its distribution is unlimited.		
11. SUPPLEMENTARY NOTES	12. SPONSORING MILITARY ACTIVITY Defense Atomic Support Agency Washington, D. C.	

13. ABSTRACT

This report describes the development of three types of on-structure stress (OSS) gages (the IF and FS soil-pressure gages and the M-1 airblast gage) based upon the load column principle. The OSS gage design is based upon the assumption (backed by theory and experiment) that if the gage is made much stiffer than the soil, the over-registration of the gage approaches a constant value. A brief discussion of some of the unique problems of measurement of soil pressures is presented. Six OSS gages (four IF, one FS, and one M-1) were statically tested and evaluated with respect to linearity, hysteresis, resolution, thermal sensitivity, and strain sensitivity. Dynamic tests were performed in a laboratory shock tube and blast load simulator facilities. The OSS gages are concluded to be adequate for soil-pressure measurements on certain types of rigid structures and for airblast measurements, even in explosive atmospheres. They successfully measured dynamic gas pressures up to 5,000 psi in the firing tubes of the laboratory blast simulator device. Additional research is recommended to evaluate the gage performance more completely in static and dynamic soil tests. A range of soil types from coarse dry sand to moist fat clays should be investigated. Future research on gages for measuring soil pressures on structures should be concentrated on development of small gages for use with models and thin-walled structures.

DD FORM 1 NOV 65 1473 REPLACES DD FORM 1473, 1 JAN 64, WHICH IS OBSOLETE FOR ARMY USE.

Unclassified

Security Classification

14. KEY WORDS	LINK A		LINK B		LINK C	
	ROLE	WT	ROLE	WT	ROLE	WT
Air burst						
Soil dynamics						
Soil pressure measurement						
Soil structure						
Stress gages						
Protective structures						
Soil stress gages						